

SYNTHESIS OF NETWORKS AND INTERPENETRATING NETWORKS
FROM FUNCTIONALIZED CASTOR AND SOYBEAN OILS

by

Şeyma Avçılar

B.S., Chemistry, Boğaziçi University, 2010

Submitted to Institute for Graduate Studies in
Science and Engineering in partial fulfillment of
the requirements for the degree of
Master of Science

Graduate Program in Chemistry

Bogaziçi University

2013

*To my beloved
Mother and Brother*

ACKNOWLEDGEMENTS

Firstly I would like to express my deepest gratitude to my thesis advisor Prof. Selim Küsefođlu for his invaluable support, encouragement and understanding. His guidance and enthusiasm has led me not only during my research, but also in business life. It was a great pleasure and chance to work with him.

I wish to express my appreciation to Prof. Duygu Avcı, Assoc. Prof. Tarık Eren for their constructive review of the final manuscript and valuable comments.

I would like to express my gratitude to all members of Chemistry Department, especially to Viktorya Aviyente, Eliza Kalvo and Hülya Metiner for their encouragement, moral support and most of all, for being a family to me. It has been a great pleasure to be among the people willing not only to transfer the knowledge, but also to share the life and help. I would like to thank to members of Küsefođlu, Nugay and Acar research groups both for their friendship and scientific help.

I am greatly indebted and thankful to Ekmel Helvacıođlu and Oruç Köklükaya for their precious friendship, moral support, encouragement and extensive scientific help, and to Dr. Cem Öztürk and Gülşah Çifci for their immense kindness, guidance, help, support and scientific help. Also, I would like to express my gratitude to Serkan Bilgili for his trust, support and kindness.

I sincerely thank to all those who have directly or indirectly helped for the work reported herein. I would like to express my gratitude to TUBITAK for supporting me for 2 years during my M.Sc. Program on the scope of the 2210-National Scholarship Program for MSc Students.

Finally I would like to express my deepest thanks to my devoted mum and my dear Ođuzhan for their endless support, encouragement, understanding and for always bearing with me and my immense gratitude to Oktay family, especially Raşit Oktay for their most valuable trust, support, kindness and encouragement.

ABSTRACT

SYNTHESIS OF NETWORKS AND INTERPENETRATING NETWORKS FROM FUNCTIONALIZED CASTOR AND SOYBEAN OILS

In this study, castor oil is maleated to give maleated castor oil (COMA). This macromonomer is capable of reacting as epoxy curing agent through its carboxylic end as well as undergoing free radical polymerization with polymerizable vinyl monomers through its double bond. The maleation of castor oil is carried out using the methodology known in literature with some small modifications increasing the maleation extent. COMA is then reacted with epoxidized soybean oil (ESO) to give a thermoset polymer ESOCOMA, as the initial network. The double bonds on maleate groups of COMA which are still intact and available to react, are then polymerized in presence of a free radical initiator to give a second interpenetrating network. This network is entirely composed of two functionalized triglycerides. Reaction of COMA and ESO with a vinyl group bearing monomer, styrene, in presence of free radical initiators resulted in a simultaneous interpenetrating network abbreviated here as Styrene-X. Another interpenetrating network is formed by using an oil based macromonomer instead of styrene, acrylated epoxidized soybean oil (AESO) to give AESO-X. All of the networks produced have considerably high oil content, especially AESO-X is unique in the sense that only the maleate and the acrylate modifications are the non-oil based portions resulting in a very high oil content of 80%. The products obtained from these reactions are all insoluble in common organic solvents so the characterization is done by FTIR. The thermal and mechanical tests such as DSC (Differential Scanning Calorimetry), DMA (Dynamic Mechanical Analysis) are carried out to further analyze the properties of the thermosets. The optimum stoichiometry for ESO/COMA is determined by surface hardness values measured by durometer whereas the effects of compositions of styrene and AESO monomers were analyzed by DMA experiments. COMA is also reacted with commercially available epoxy resins to give clear, tough, high tensile strengths thermosets. The optimization and characterization studies of COMA as an epoxy curing agent are currently in progress.

ÖZET

FONKSİYONALİZE EDİLMİŞ HİNT YAĞI VE SOYA FASULYESİ YAĞLARINDAN AĞ VE GİRİŞMİŞ AĞ YAPISI SENTEZİ

Bu çalışma kapsamında hint yağı ile maleik anhidritin esterleşme tepkimesi ile maleinize hint yağı elde edilmiştir (COMA). Bu makromonomer, karboksil ucu ile epoksi gruplarıyla epoksi halka açılması, polimerize olabilir çift bağı ile de radikal polymerizasyon reaksiyonları verebilir. Maleat modifiye hint yağı (COMA), literatürde daha önce bilinen yöntemlere maleatlanma yüzdesini ve verimi artırmak için yapılan ufak modifikasyonlar sonucu elde edilmiştir. COMA'nın epokside soya yağı (ESO) ile reaksiyonu sonucunda ilk ağ dokusu olarak termoset bir polimer (ESOCOMA) sentezlenmiştir. COMA'nın maleat grubu üzerindeki çift bağların serbest radikal reaksiyon başlatıcılar kullanılarak tepkimesi sonucunda ise girişmiş bir ağ dokusu elde edilmiştir. Bu ağ dokusu, monomerleri sadece trigliserit olan bir girişmiş ağ dokusudur. COMA molekülündeki çift bağların polimerleşebilme özelliğinden yararlanmak amacıyla ESOCOMA reaktif seyreltici stiren ile karıştırılarak serbest radikal başlatıcılar ile eş zamanlı girişmiş ağ yapılı termoset sentezlenmiştir. Bir başka ağ yapılı termoset, stiren yerine bitkisel yağ türevli bir makromonomer, akrilik epoksi soya yağı (AESO) kullanılarak sentezlenmiştir (AESO-X). Elde edilen polimerler yüksek yağ içeriklerine sahiptir. Özellikle AESO-X, 3 bileşeni de trigliserit kökenli, %80'lere varan çok yüksek yağ içeriğine sahip bir termostettir. Çalışmada üretilen tüm polimerlerin karakterizasyon çalışmaları, organik çözücülerde çözünmemeleri sebebiyle yalnızca FTIR kullanılarak yapılmıştır. Termal ve fiziksel davranışları DSC ve DMA kullanılarak karakterize edilmiştir. COMA'nın ticari epoksi reçinelerle reaksiyonu sonucu yüksek toklukta, yüksek mekanik mukavemetli homojen termosetler elde edilmiştir. COMA'nın epoksi kurlenme maddesi olarak ticarileşmesi için optimizasyon ve karakterizasyon çalışmaları sürdürülmektedir.

TABLE OF CONTENTS

ACKNOWLEDGEMENTS	iv
ABSTRACT.....	v
ÖZET	vi
LIST OF FIGURES	x
LIST OF TABLES	xii
LIST OF ACROYNMS/ABBREVIATIONS	xiii
1. INTRODUCTION	1
1.1. Significance of Renewable Raw Materials for Chemical Industry	1
1.2. Natural Oils	2
1.2.1. Structure and Properties of Fatty Acid and Triglycerides	2
1.2.2. Structure and Properties of Castor Oil.....	4
1.2.3. Structure and Properties of Soybean Oil	6
1.3. Chemistry of Triglycerides.....	7
1.3.1. Reactions at the Carboxy Functional Group of Triglycerides.....	8
1.3.2. Reactions at the Unsaturated Fatty Acid Chain.....	8
1.4. Maleation of Castor Oil.....	10
1.5. Ring Opening Polymerization of Epoxidized Soybean Oil	11
1.6. Interpenetrating Polymer Networks	12
2. RESEARCH OBJECTIVES	14
3. EXPERIMENTAL.....	16
3.1. Materials and Apparatus.....	16
3.1.1. Materials	16

3.1.2. Apparatus.....	16
3.2. Synthesis of Maleated Castor Oil (COMA, 2)	17
3.3. Ring Opening Polymerization of Epoxidized Soybean Oil with Maleated Castor Oil (ESOCOMA, 4)	18
3.4. Self-Crosslinking of ESOCOMA network (5).....	18
3.5. Simultaneous Interpenetrating Polymer Networks with ESOCOMA.....	19
3.5.1. ESOCOMA-St Network (6)	19
3.5.2. ESO-COMA-AESO Network (8).....	19
4. RESULTS AND DISCUSSION.....	20
4.1. Characterization of COMA (2)	20
4.1.1. Spectral Identification	21
4.1.2. Determination of Maleation Ratio by NMR Spectrum	23
4.2. Characterization of ESOCOMA (4).....	24
4.2.1. Spectral Identification of ESOCOMA (4).....	26
4.2.2. Thermal and Mechanical Properties of ESOCOMA (4)	27
4.3. Characterization of self-crosslinked ESOCOMA (selfX) (5)	28
4.3.1. Spectral Identification of selfX (5).....	28
4.3.2. Thermal and Mechanical Properties of selfX (5)	30
4.4. Characterization of Simultaneous Interpenetrating Network of Styrene-X (6) ..	31
4.4.1. Spectral Identification	34
4.4.2. Mechanical Properties	35
4.5. Characterization of Simultaneous Interpenetrating Network of AESO-X (8)	40
4.5.1. Spectral Identification	42
4.5.2. Mechanical Properties	42
4.6. Comparison of Thermal Properties for all adducts	45
4.7. Reaction of COMA with commercial epoxy resins	46

5. CONCLUSION..... 48

REFERENCES 49

LIST OF FIGURES

Figure 1.1.	Feedstock for chemical industry [2].	2
Figure 1.2.	Structure of a triglyceride molecule.	3
Figure 1.3.	Structure of ricinoleic acid (C ₁₈ H ₃₀ O ₃) (one fatty acid chain).	4
Figure 1.4.	Structure and reactivity of castor oil (Courtesy of CashChem, Inc.) [4].	5
Figure 1.5.	Fatty acids in soybean oil.	6
Figure 1.6.	Possible transformations of the functional groups on a representative fatty acid chain.	7
Figure 1.7.	Epoxidation of unsaturated triglyceride.	9
Figure 1.8.	Maleation of castor oil.	11
Figure 2.1.	Synthesis and polymerization of triglyceride based adducts.	15
Figure 4.1.	Maleation of Castor Oil.	20
Figure 4.2.	IR Spectra of Castor Oil (1) and Maleated Castor Oil (2).	21
Figure 4.3.	¹ H - NMR spectrum of COMA (2).	22
Figure 4.4.	Epoxidation of Soybean Oil.	24
Figure 4.5.	Reaction of COMA with ESO.	25
Figure 4.6.	IR Spectrum of ESOCOMA.	26
Figure 4.7.	DSC Analysis graph of ESOCOMA (4).	27
Figure 4.8.	DMA Graph of ESOCOMA (4).	27
Figure 4.9.	Self Crosslinking reaction of ESOCOMA.	28

Figure 4.10.	IR spectra of SelfX, pre and post reaction.....	29
Figure 4.11.	DSC Analysis graph of selfX(5).	30
Figure 4.12.	DMA Graph of selfX(5).	30
Figure 4.13.	Synthesis of Simultaneous IPN of ESO-COMA-Styrene.	32
Figure 4.14.	IR Spectrum of Styrene-X Network (6).	34
Figure 4.15.	DMA Graph of Styrene-X 1.5 : 0.25.....	35
Figure 4.16.	DMA Graph of Styrene-X 2.0 : 0.25.....	35
Figure 4.17.	DMA Graph of Styrene-X 2.5 : 0.25.....	36
Figure 4.18.	DMA Graph of Styrene-X 3.0 : 0.25.....	36
Figure 4.19.	DMA Graph of Styrene-X 1.5 : 0.10.....	38
Figure 4.20.	DMA Graph of Styrene-X 1.5 : 0.20.....	38
Figure 4.21.	DMA Graph of Styrene-X 1.5 : 0.30.....	39
Figure 4.22.	Synthesis of simultaneous IPN of ESO-COMA-AESO.....	41
Figure 4.23.	IR Spectrum of AESO-X Network.....	42
Figure 4.24.	DMA Graph of AESO-X 1.5 : 0.15.....	43
Figure 4.25.	DMA Graph of AESO-X 1.5 : 0.30.....	43
Figure 4.26.	DMA Graph of AESO-X 1.5 : 0.40.....	44
Figure 4.27.	DSC Analysis graph for all adducts.	46

LIST OF TABLES

Table 1.1.	Fatty acid distribution of some common oils.	3
Table 1.2.	Properties of Castor Oil [5].....	4
Table 1.3.	The general properties of soybean oil [9].	7
Table 4.1.	Surface Hardness Values for Optimization of COMA/ESO Ratio.....	25
Table 4.2.	Result of mechanical analysis for selfX (5).....	31
Table 4.3.	Composition of Styrene-X Network-Constant weight % styrene.....	32
Table 4.4.	Composition of Styrene-X Network-Constant ratio for COMA/ESO.....	32
Table 4.5.	Result of mechanical analysis for Styrene-X (6) Adducts.....	39
Table 4.6.	Composition of AESO-X Network- Constant ratio for COMA/ESO.	40
Table 4.7.	Result of mechanical analysis for AESO-X (8) Adducts.	45

LIST OF ACROYNMS/ABBREVIATIONS

ADMET	Acyclic Diene Metathesis
AESO	Acrylated Epoxidized Soybean Oil
AMC II	Commercial catalyst (Cr(III) carboxylate)
ATR-IR	Attenuated Total Reflectance Infrared
BPO	Benzoylperoxide
COMA	Maleated Castor Oil
DMTA	Dynamic Mechanical Thermal Analysis
DSC	Differential Scanning Calorimeter
ESO	Epoxidized Soybean Oil
HDPE	High Density Polyethylene
IPN	Interpenetrating Network
IR	Infrared
MESO	Monomethyl Maleated Epoxidized Soybean Oil
NMR	Nuclear Magnetic Resonance
PVC	Poly(vinylChloride)
T _g	Glass Transition Temperature
TGA	Thermogravimetric Analyses
THF	Tetrahydrofuran
UV	Ultraviolet

1. INTRODUCTION

1.1. Significance of Renewable Raw Materials for Chemical Industry

The demand for the renewable plant-based chemicals as raw materials for the chemical industry is increasing. The use of plant based polymers as opposed to the petroleum based ones is increasing as the plastics industry begins to produce polymers with better and more interesting properties from plant based materials. The plant oils serve as very suitable raw materials since they are produced all over the world and are cheap and easily replenished annually. Moreover, plant oils have the potential to replace petroleum based materials with equal or better physical properties of the end-products. The very early studies on polymer synthesis with plant oils have resulted in low molecular weight and low structural strength-products; however recent studies show that the plant oils have the potential to take a major part in thermosetting polymer production. The growing interest and the increase in the research on plant oil derived polymers have resulted in manufacture of many thermosetting polymers exhibiting the required physical and mechanical qualities such as rigidity, strength, glass transition temperature [1].

The industrial revolution has brought about changes not only in the processes of manufacturing and production, but also on the choices of raw materials. Before the revolution, the plant and animal based sources were widely used as industrial materials however after the revolution the increases in population and mass production requirements gave rise to replacement of these with coal, and then with petroleum, following the developments in petroleum refining procedures. Figure 1.1 shows the utilization of the sources over the last 200 years. As could be seen from the figure, today, petroleum continues to predominate over the other sources.

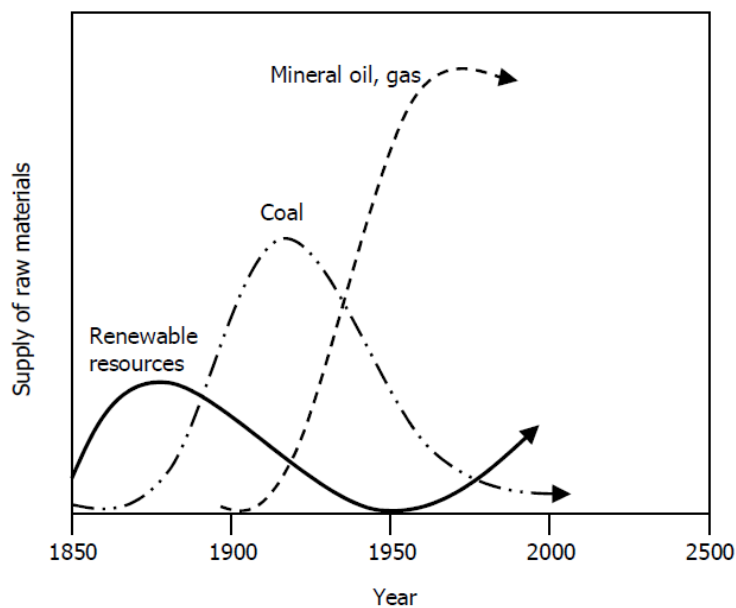


Figure 1.1. Feedstock for chemical industry [2].

1.2. Natural Oils

1.2.1. Structure and Properties of Fatty Acid and Triglycerides

Lipids or fats are a group of naturally occurring chemicals with molecular weights varying from 750 to 1000. Vegetable oils, called triglycerides, are composed of three fatty acid groups bonded via an ester linkage to a glycerol unit. In nature, lipids have been derived from various sources such as vegetables, animals or marine sources. Lipids have been used as nutrients through the ages and more recently as fuel, lubricant and starting material for synthesis of other chemicals. Such a wide application area could be explained with the unique chemical structure and physical properties which gives rise to many functionalities and variety of chemical reactions. In addition, the properties of the fat may differ due to the combination of different fatty acids that are esterified at the three hydroxyl ends of glycerol. A general structure of triglyceride molecule is shown below.

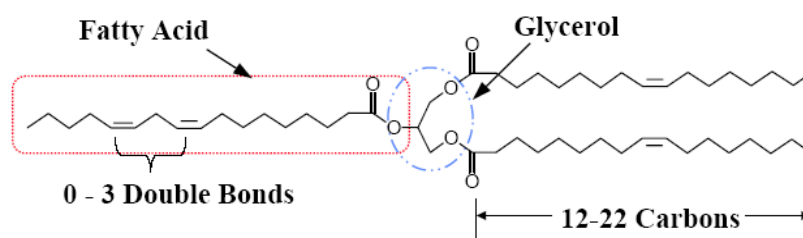


Figure 1.2. Structure of a triglyceride molecule.

Chain lengths of fatty acids may vary from 2 to 80 carbons, 16, 18, 20 being the most abundant numbers. Unsaturated sites may exist up to a number of 3 commonly appearing at the 9, 12, 15th carbons. These double bonds are generally non-conjugated and in the cis geometry. The main reactive functional groups of fatty acids are double bonds, allylic positions, and carboxyl groups. There are also rare triglycerides that contain some other functionalities with substituents such as fluoro (fish oil), dicarboxylic (plant cuticles), divinyl ether (potato leaves), isomeric epithio (canola oil), nitrate (human plasma), hydroxyl (castor oil), keto (Licania seed oil) and epoxy groups (vernonia oil) [3].

The distribution of fatty acids in a given type of oil may vary with different time of harvest, origin of plantation, soil and subspecies of plant. The knowledge of the distribution serves as a very important tool for further modifications and addition of functionalities which will be of help in synthesis. Table 1.1 shows the average fatty acid distribution of some common vegetable oils. Genetically engineered plants made it possible to fully control the fatty acid distribution and to introduce new and exotic fatty acids to triglyceride structures.

Table 1.1. Fatty acid distribution of some common oils.

Vegetable Oil	Fatty Acid %						
	Palmitic Acid	Stearic Acid	Oleic Acid	Linoleic Acid	Linolenic Acid	Ricinoleic Acid	Other
Castor Oil	1.5	0.5	5	4	0.5	87.5	-
Soybean Oil	10	4	25	55	6	-	-
Linseed Oil	5	4	22	17	52	-	-
Sunflower Oil	6	4	42	47	1	-	-
Palm Oil	39	5	45	9	-	-	2
Rappeseed Oil	4	2	56	26	10	-	2

1.2.2. Structure and Properties of Castor Oil

Castor oil is also known as ricinus oil, oil of Palma Christi, tangan-tangan oil, and neoloid. Just like most of the vegetable oils and fats, castor oil is a triglyceride of various fatty acids. However, it is unique due to very high (87–90 wt %) content of ricinoleic acid, $C_{18}H_{34}O_3$, structurally *cis*-12-hydroxyoctadeca-9-enoic acid, an eighteen-carbon hydroxylated fatty acid having one double bond. Castor oil, sometimes described as a triglyceride of ricinoleic acid, is one of the few commercially available glycerides that contain hydroxyl functionality in such a high percentage of one fatty acid [4].

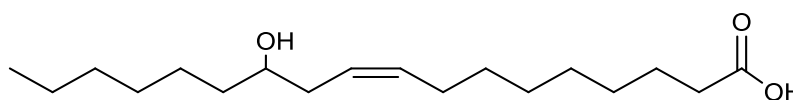


Figure 1.3. Structure of ricinoleic acid ($C_{18}H_{30}O_3$) (one fatty acid chain).

Castor oil differs from the other triglycerides by its high specific gravity, viscosity, and hydroxyl value as well as by another unique feature that is alcohol solubility: one volume of castor oil dissolves in two volumes of 95% ethyl alcohol at room temperature, and the oil is miscible in all proportions with absolute ethyl alcohol. Castor oil is soluble in polar organic solvents, however less soluble in aliphatic hydrocarbon and other nonpolar organic solvents and has a slight solubility in petroleum ether, which is a characteristic feature distinguishing it from other fats.

Table 1.2. Properties of Castor Oil [5].

CAS No	8001-79-4
Color	Nearly Colorless or Faintly Yellow
Relative Density at 20°C	0.952-0.965
Moisture	0.3% max.
Iodine Value	82-90
Saponification Value	176-187
Acid Value	2.0 max.
Unsaponifiables w/w	0.8% max.
Optical Rotation	between +3.5° and 6.0°
Hydroxyl Value	150 min.
Peroxide Value	5.0 max
Light Absorption	1.0 max

Castor oil is normally pale yellow, highly viscous, and has a slight characteristic odor, however, the oil can vary in color depending on the method of recovery and blending to meet specifications. Normally, it is pale yellow, highly viscous and nearly tasteless oil, and has a slight characteristic odor. However, due to the presence of a toxic protein, ricin and its minor use as a cathartic agent, the harvesting, storage and extraction of castor oil beans require some precautions.

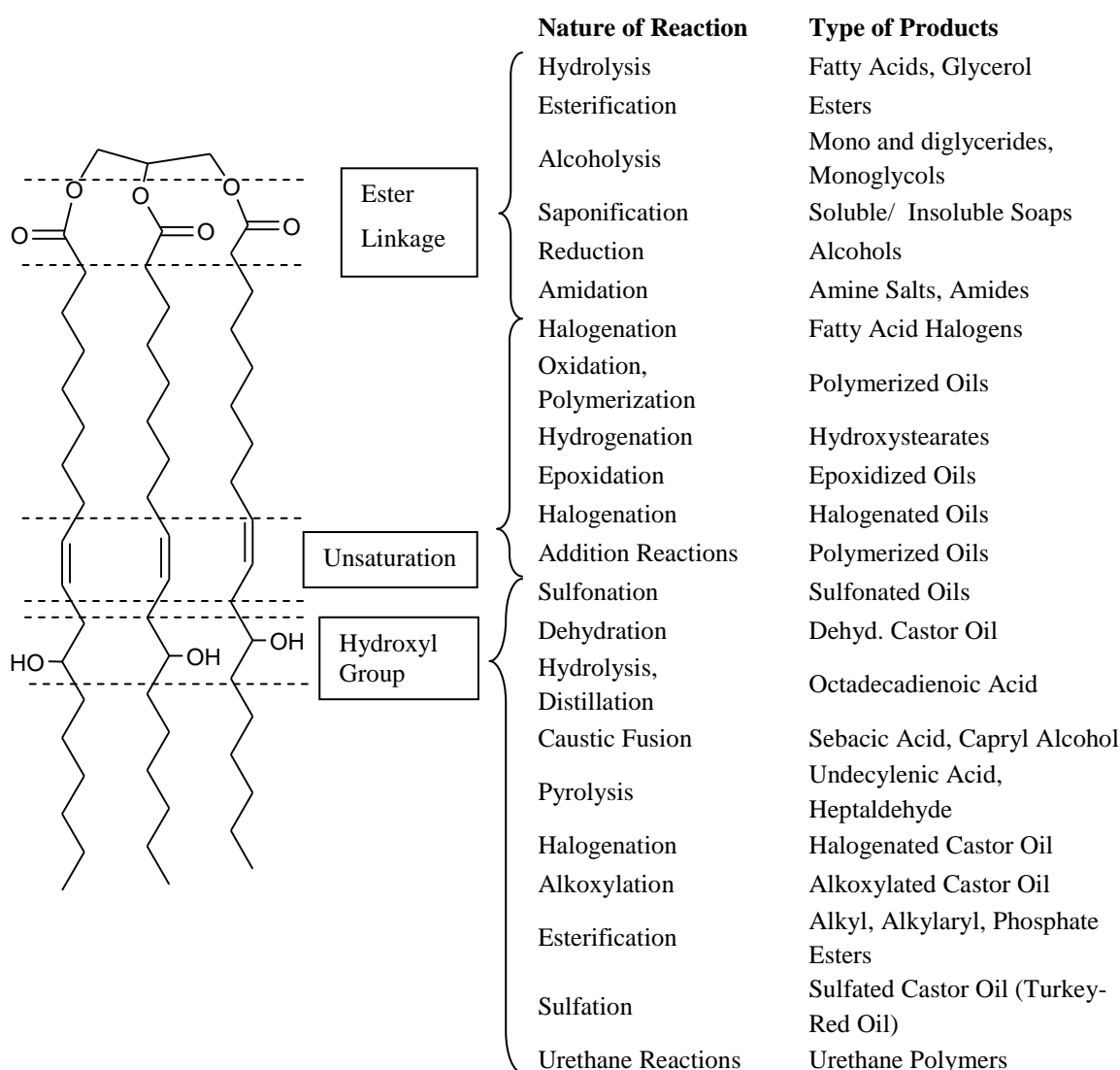


Figure 1.4. Structure and reactivity of castor oil (Courtesy of CashChem, Inc.) [4].

The major end-use industries for castor oil derivatives castor oil are:

- Lubricants & Greases

- Coatings
- Personal Care & Detergent
- Surfactants
- Oleochemicals

Castor oil serves as an industrial raw material for the manufacture of a number of complex organic derivatives [6-8].

1.2.3. Structure and Properties of Soybean Oil

Soybean oil is a mixture of glycerol esters of unsaturated oleic, linoleic and linolenic acids and saturated palmitic and stearic acids and has an average of 4.2 double bonds per triglyceride molecule.

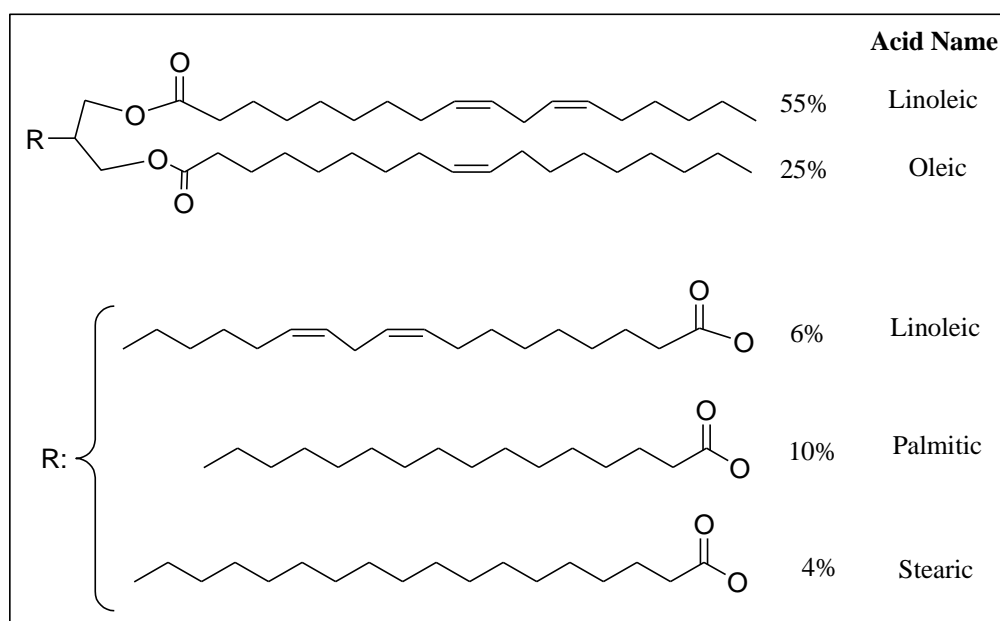


Figure 1.5. Fatty acids in soybean oil.

Soybean oil is one of the most preferred as a renewable feedstock in chemical industry since it is produced in high amounts and it has high level of unsaturation, though

those double bonds are relatively unreactive, thus some functionalization or chemical transformations are required before use as a monomer in polymerization reactions.

Table 1.3. The general properties of soybean oil [9].

Iodine Number	117-140
Saponification Number	189-195
Viscosity(cP) at 40 °C	28
Smoke Point	213 °C
Flash Points	317 °C
Fire Point	342 °C
Density(15 °C)	0.910-0.934
Molecular Weight (g/mole)	850-870

1.3. Chemistry of Triglycerides

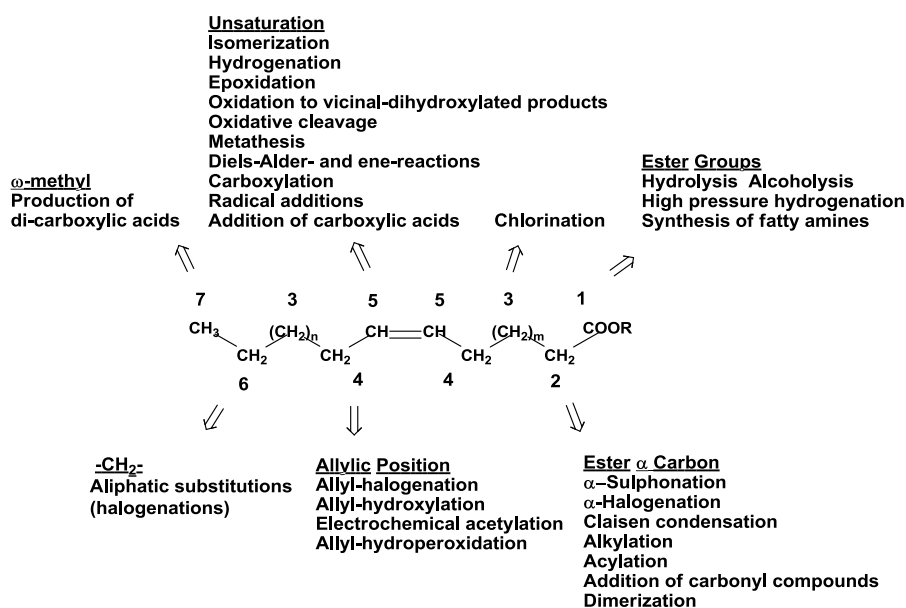


Figure 1.6. Possible transformations of the functional groups on a representative fatty acid chain.

There are mainly six reactive sites appropriate for chemical modifications. Those active sites are ester group (1), α position to the ester group (2), methylene groups (3, 6), allylic carbons (4), unsaturated carbon-carbon double bonds (5), ω -methyl (7) as shown in

figure below. These sites are the potentially reactive sites which could be utilized for introduction of polymerizable groups on triglyceride molecules [10].

1.3.1. Reactions at the Carboxy Functional Group of Triglycerides

The main and widely utilized reactions on the carboxy groups of esters are the hydrolysis, transesterification, fatty alcohol synthesis via high pressure hydrogenation and fatty amine synthesis. The hydrolysis of esters gives fatty acids which may be further reacted to yield fatty amides, whereas the alkaline hydrolysis of esters yields alkali soaps, which is a very basic and most common method dating back to the year 2800 BC in Ancient Babylon. The reduction of fatty acid esters under high pressure gives the corresponding fatty alcohol. In addition to those, one of the most widely used reaction is the transesterification of fatty esters with methanol to produce methyl esters (used as biodiesel) and glycerol [11].

1.3.2. Reactions at the Unsaturated Fatty Acid Chain

The unsaturated parts on a fatty acid chain are the most reactive and easily modified of all. The most well-known and common reactions are hydrogenation, epoxidation, oxidative scission, carboxylation, Diels-Alder, olefin metathesis, cross metathesis and dimerization reactions. Since double bonds are more susceptible to oxidative decomposition than carbon-carbon single bonds, hydrogenation of the double bond is used in order to improve oxidative stability, shelf life, maintain color stability and to raise melting point of unsaturated fatty esters. Hydrogenation is generally carried out in presence of nickel, platinum and palladium catalysts for industrial hydrogenation of oils, yielding margarine.

Epoxidation is one of the most important reactions of the unsaturated fatty acid chains. The epoxidation reaction of an unsaturated triglyceride with hydrogen peroxide in presence of formic acid catalyst is shown below in Figure 1.6.

The epoxidation is commonly utilized because three-membered and strained epoxy ring is very susceptible to nucleophilic ring opening reaction. The most abundant reactions are the reaction of epoxides with water to produce vicinal diol, alcohol to hydroxy ether, carboxylic acid to hydroxyl ester, hydrogen sulfide to mercapto alcohol, primary and secondary amines to amino alcohol, monoprotic halogen acids to chloro-, bromo- and iodohydrins [12]. Epoxidized oils and the ketonized oils obtained by the rearrangement of those epoxidized oils are used as plasticizer for PVC [13] and HDPE. In addition, vicinal diols produced by water hydrolysis is utilized in manufacture of biodegradable polyurethane foam.

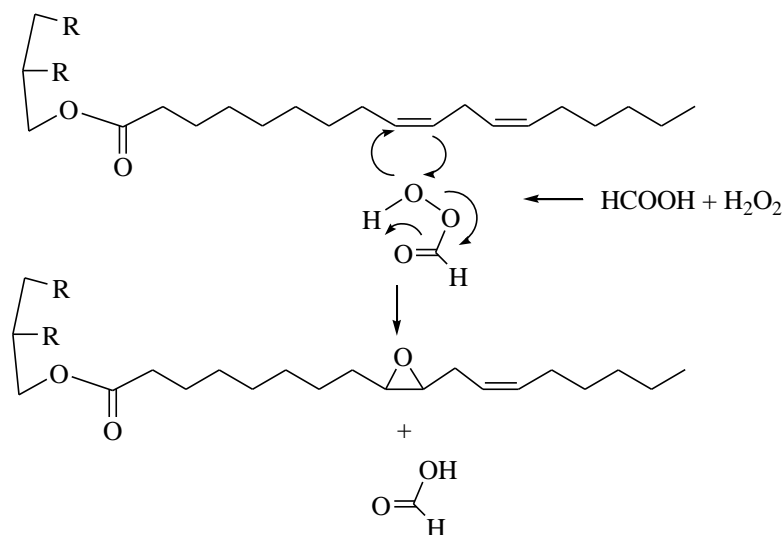


Figure 1.7. Epoxidation of unsaturated triglyceride.

One other successful example to nucleophilic ring opening of epoxidized soybean oil is the Acrylated Epoxidized Soybean Oil (AESO) produced with acrylic acid ring opening of ESO. AESO can undergo free radical polymerization with reactive diluents such as styrene to give thermoset resins with mechanical properties that are similar to commercially successful polyester and vinyl ester resins [14, 15].

Öztürk et al. reported a new polymerizable triglyceride based monomer produced via addition of 4-vinylbenzene sulfonic acid to epoxidized soybean oil triglycerides. This monomer undergoes free radical homopolymerization as well as copolymerization with styrene and polymerization via acyclic diene metathesis (ADMET) which is a

polymerization technique using metathesis of terminal dienes to produce linear polymers and ethylene with step-growth kinetics [16].

Wallenberger et al. synthesized a broad range of crosslinked polyesters by curing epoxidized soybean oil with various dicarboxylic acid anhydrides in the presence of cure catalysts such as tertiary amines, imidazoles, or aluminum acetylacetonate. The mechanical and thermal properties of the casting resins were determined to depend upon the type of anhydride. The anhydrides of hexahydrophthalic acid, succinic acid, and norbornene dicarboxylic acid yielded highly flexible rubbery materials with glass transition temperatures below room temperature whereas more rigid anhydrides of maleic and phthalic acid resulted in amorphous stiff polyesters with higher glass transition temperatures varying between 43 and 73 [17].

1.4. Maleation of Castor Oil

As previously mentioned there exist many reactive sites on castor oil structure. The β -positioned hydroxyl group reacts like an ordinary secondary alcohol and can be esterified as well as undergo elimination, allylic bromination giving rise to halohydrin formation etc. [18]. Thus, the presence of hydroxyl groups and double bonds makes the oil suitable for many reactions and modifications.

Can et al. modified the castor oil with both aliphatic alcohols, such as glycerol and erythritol, and an aromatic alcohol, bisphenol A propoxylate. The alcoholysis products were malinated and free radically polymerized with styrene. In addition direct malination of castor oil, skipping the alcoholysis step, has been carried out in order to determine the effect of alcoholysis on the properties of final product, castor oil based resins [19].

Wang et al. prepared biodegradable plastic foams with a high content of castor oil. First, castor oil has been maleated to produce maleated castor oil without using any catalyst. Then plastic foams were synthesized via free radical polymerization of the maleate unsaturation using the reactive diluent styrene as co-monomer [20].

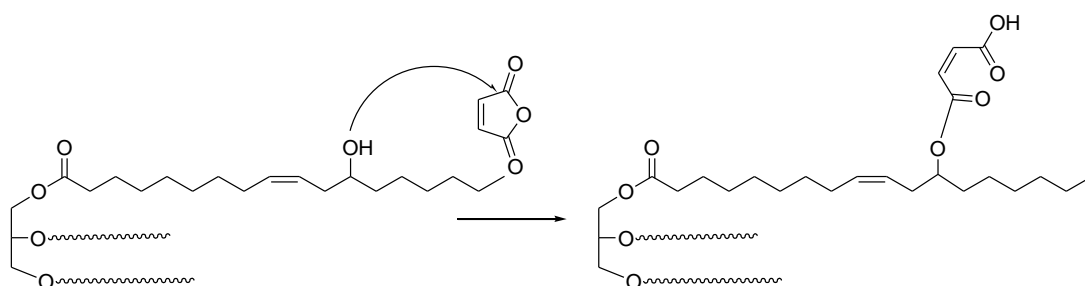


Figure 1.8. Maleation of castor oil.

US Patent 6,225,485 reports the direct and efficient method for maleation of castor oil with no by-products. The reaction is carried out without any catalyst. The reaction time is 7-8 days in order to increase the conversion, while decreasing the reaction temperature to 50 °C for the last 6 days of this time period. The end product is utilized in several industrial applications such as hardening agent in epoxy resins, leather fat liquoring as emulsifiers for polymerization of vinyl chloride and flexibilizing agents of epoxy resins [21].

1.5. Ring Opening Polymerization of Epoxidized Soybean Oil

The epoxy group on fatty acid chain reacts readily with nucleophilic reagents. The reactions with water and alcohol produce diols and alkoxy alcohols respectively whereas the ring opening with carboxylic acid results in hydroxyl ester.

US Patent 6,121,398 describes the reaction of acrylic acid with epoxidized soybean oil to yield acrylated epoxidized soybean oil. The resulting product AESO could be polymerized with or without reactive diluents such as styrene via free radical mechanism to give thermoset resins with mechanical properties similar to commercial polyester and vinyl ester resins [14].

Another example to the reaction of epoxidized soybean oil with carboxylic acid and/or alcohols is the use of it as a chain extender in unsaturated polyester synthesis. The utilization of ESO decreases the time span of the condensation reaction without any loss in thermal and mechanical properties of the material [22].

The reaction of ESO with cinnamic acid in presence of triphenyl phosphine as a catalyst has been carried out to give cinnamate ester of epoxidized soybean oil which could be photopolymerized with styrene, vinyl acetate, methylmetacrylate or by itself via free radical mechanism to yield polymers with different mechanical properties [23].

In addition to those, Esen et al. has synthesized the monomethyl maleated epoxidized soybean oil (MESO) reacting monomethyl maleate with ESO in presence of AMC-2 catalyst. Then, MESO has been photopolymerized with UV light and was free radically homopolymerized and copolymerized with styrene, vinyl acetate, and methyl methacrylate [24, 25].

1.6. Interpenetrating Polymer Networks

Interpenetrating network materials are basically defined as “two or more polymers in a network form with at least one polymer that is polymerized or cross-linked in the immediate presence of the other”. An interpenetrating network may turn out to be highly useful and efficient since it has the potential to exhibit and combine the properties of two different crosslinked systems of which it is derived. There are two major types of interpenetrating networks, sequential and simultaneous interpenetrating network. Sequential IPNs are produced in two steps, one crosslinked network is prepared and the second network is obtained by a subsequent swelling of the first network with the new monomer followed by the polymerization then further crosslinking of the newly introduced monomer. Simultaneous IPNs involve the mixing of all components in one step while independent reactions proceed simultaneously within the same reaction vessel.

There are proposed more terms to fully define different types of IPN systems. Semi-IPN and pseudo-IPN refer to interpenetrating polymer networks in which one of the polymers is not crosslinked for sequential and simultaneous synthesis, respectively. Interpenetrating polymer networks could be used for systems where the pair of reactions proceeds either via step polymerization systems or chain polymerization systems, or as a combination of both.

Sperling et al. synthesized several interpenetrating network based on a castor oil polyurethane model, where the hydroxyl groups were reacted with 2,4-toluene diisocyanate for polyurethane formation whereas the second network was formed with polymerization of styrene and divinylbenzene both sequentially and simultaneously. The mechanical properties of IPNs and semi interpenetrating networks have been determined and modulus-temperature, stress-strain and impact resistance studies have shown variation depending on the compositions [26].

There are some IPNs commercially utilized, however not identified as such. The inclusion of a thermoplastic into an unsaturated polyester system for the sake of decreasing the shrinkage during crosslinking or the increase in toughness and resilience of unsaturated polyesters obtained via addition of polyurethanes are some examples to the commercial applications. Some other examples are epoxy resin-polysulfide, epoxy resin-polyester, epoxy resin-polyurethane, polyurethane-poly(methyl methacrylate), polysiloxane-polyamide, and epoxy resin-poly (diallyl phthalate) systems. However, those systems do not fit to the basic definition of a standard IPN, owing to the presence of grafting and crosslinking between the two components and violating the rule “no covalent bond between two separate networks”. Nevertheless, this situation is an advantage as it leads to IPNs with minimal phase separation which is always a challenge in IPN s [27].

2. RESEARCH OBJECTIVES

In this work, the hydroxyl group on ricinoleic acid will be reacted with maleic anhydride to give castor oil-maleic anhydride adduct (COMA, 2). Castor Oil contains 2.44 hydroxyl groups per triglyceride and in principle all of them can be reacted with maleic anhydride. Maleate unsaturation is preserved during this reaction as well as the unsaturation on backbone of the castor oil. Figure 2.1 shows the reaction of one hydroxyl group with maleic anhydride for simplicity, however one should keep in mind that the other hydroxyl groups also give the same reaction.

In the next step COMA will be reacted with epoxidized soybean oil (ESO, 3) where the carboxyl end of COMA opens the epoxy groups of ESO. As ESO has, on average, 4.2 epoxy group per triglyceride, the resulting adduct (ESOCOMA, 4) is a highly crosslinked network. In the next step the maleate unsaturation of the ESOCOMA network will be free radically polymerized either alone or with another olefinic monomer to provide interpenetrating network (IPN). For the second network, the participation of the unsaturation on castor oil is also possible.

IPN preparation will be done both sequentially and simultaneously using styrene and acrylated epoxidized soybean oil (AESO, 7) as the co-monomer as shown in Figure 2.1. The latter adduct has the unique property that all components of the both networks are oil based ensuring a very high oil content.

Finally, the chemical, mechanical and thermal properties of the resulting IPNs will be examined.

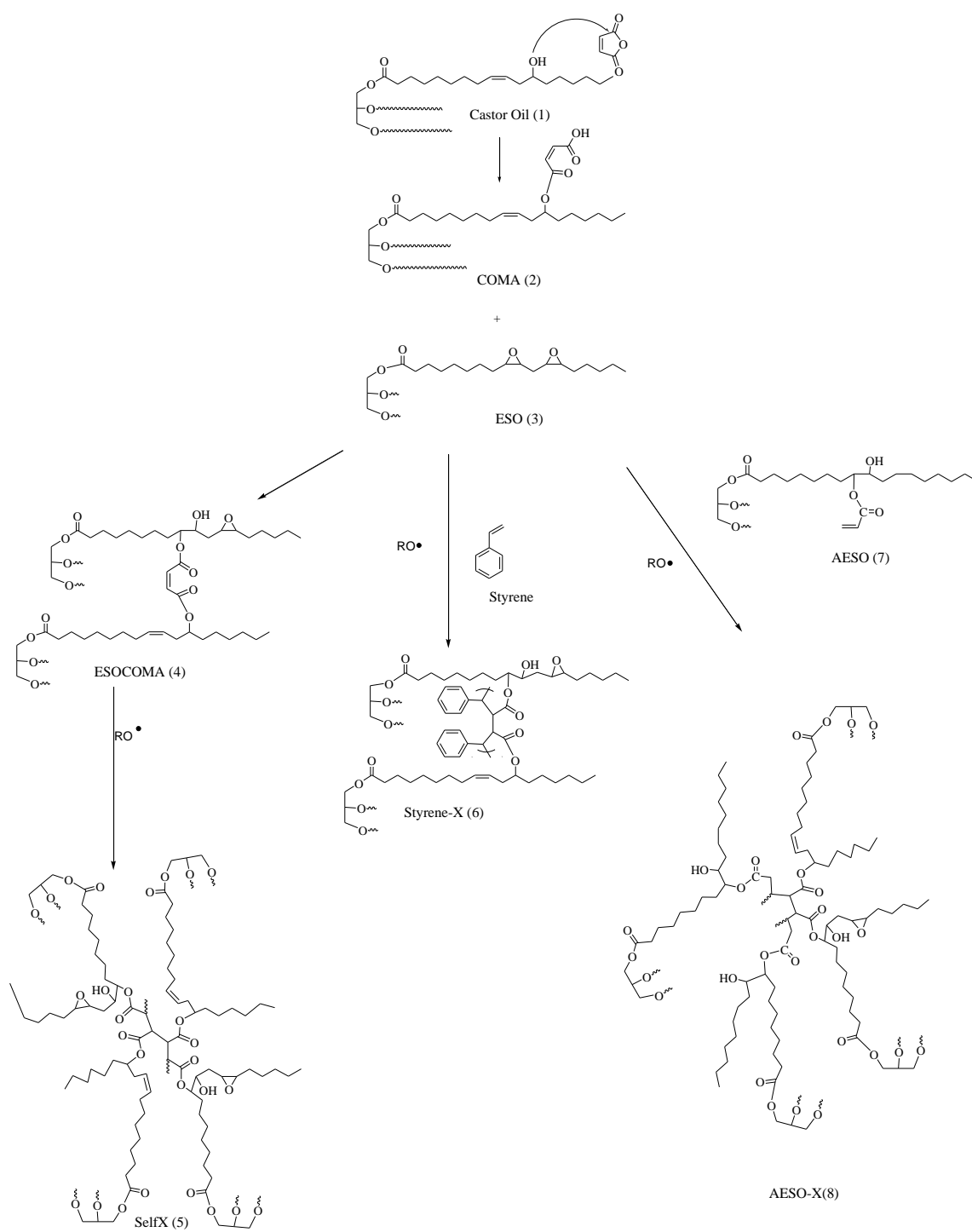


Figure 2.1. Synthesis and polymerization of triglyceride based adducts.

3. EXPERIMENTAL

3.1. Materials and Apparatus

3.1.1. Materials

Castor Oil was purchased from Şifa Kimya, maleic anhydride was supplied by Cam Elyaf A.Ş. and epoxidized soybean oil, acrylated epoxidized soybean oil were supplied by Frimpeks A.Ş. all of Istanbul, Turkey. Styrene was purchased from Merck (Germany), THF was purchased from J.T.Baker (Deventer Holland), CH₂Cl₂ was supplied by Cakir Kimya (Istanbul, Turkey), CDCl₃ was purchased from Merck (Germany), and used for ¹H NMR analysis.

3.1.2. Apparatus

The IR analysis was performed on a Nicolet 380 FT-IR with Smart Diamond ATR. All the ¹H NMR spectra were recorded on a Varian 400-MHz NMR instrument operating at a frequency of 399.986 MHz for proton. The spectra were reported as ppm (δ) with TMS as internal standard.

DSC characterization was performed by “Thermal Analyses” Q 200 instrument with a 10 °C/min heating rate. DSC samples were prepared by weighing 7–9 mg of polymer samples in aluminum DSC pans. Temperature scans were run for polymers from -50 °C to 200 °C.

The dynamic mechanical thermal analysis of the polymer samples were performed by using TA Instrument Q800 Dynamic Mechanical Analyzer (DMA) in single cantilever mode. Temperature scans were run at a heating rate of 3 °C/min with a vibration frequency of 1 Hz. Temperature scans were run from -50 °C to 100 °C for polymers numbered 4, 5, 8

and from -50 °C to 150 °C for polymers numbered 6. The average dimensions ($t \times w \times l$) of the samples were $2 \pm 0.2 \times 12 \pm 0.2 \times 35 \pm 0.2 \text{ mm}^3$.

The Zwick/Roell Durometer (Ulm, Germany) with Shore A was used to determine the surface hardness of polymer samples; the test was performed according to ASTM D 2240 standard test. The average dimensions ($t \times w \times l$) of the samples were $7 \pm 0.2 \times 12 \pm 0.2 \times 35 \pm 0.2 \text{ mm}^3$ and analyses have been done at room temperature (25 °C). Hardness values range from 0 - for full penetration to 100 - for no penetration. To obtain a reliable analysis data, the samples were tested at least at 10 different points on the same surface.

3.2. Synthesis of Maleated Castor Oil (COMA, 2)

COMA was synthesized according to the procedure given in literature (20) with some modifications. Thus, in a N_2 purged flask equipped with a magnetic stirrer and sealed with a rubber septum, 49.8 g (53.4 mmol) castor oil and 13.6 g (13.9 mmol) maleic anhydride were mixed at room temperature. 50 mL toluene was added to the mixture. The mixture was heated to 100 °C and kept at that temperature for 3-5 days, then at 50 - 60 °C for 2-3 days. Afterwards, toluene was evaporated under vacuum and during this step the un-reacted maleic anhydride sublimed out and was removed. The final product is a yellow viscous liquid. The characterization has been carried out with IR and NMR.

IR Spectrum (cm^{-1}): 3007.67 (C=C-H stretching), 2925.78, 2854.87, and 1456.56 (C(sp^3)-H stretching), 1731.51 (C=O stretching), 1632.44 (-C=C stretching), 1413.73, 978.26 (C(=O)-O-H bend), 817.75 (=C-H bend), 1209.84 (C-C(=O)-O stretching).

^1H NMR (CDCl_3 , 400 MHz) ppm: 0.9 (-CH₃), 1.2–1.6 (-CH₂-),c 2.3 (-CH₂-(C=O)-), 3.6 (-O-H), 4.1–4.2 (-CH₂-O-(C=O)-), 5.0 (-CH-O-(C=O)-), 5.2–5.6 (-CH=CH-), 6.1– 6.4 (-CH=CH-, maleate)

3.3. Ring Opening Polymerization of Epoxidized Soybean Oil with Maleated Castor Oil (ESOCOMA, 4)

3.0 grams of epoxidized soybean oil was mixed with 4.5 g of COMA and well stirred. The mixture was cast into a Teflon mold and kept at room temperature for 4-5 hrs to release air bubbles. Vacuum may be utilized at that stage, if desired. The mold was heated at 80 °C for 4 hrs. Transparent yellow colored thermosets were obtained. Characterization was carried out with IR analysis. The sample is insoluble in organic solvents.

IR Spectrum (cm^{-1}): 3521.50 (**O-H**), 3010.88 (**C=C-H** stretching), 2924.27, 2854.21, and 1458.82 (**C** (sp^3)-**H** stretching), 1735.51 (**C=O** stretching), 1643.49 (**-C=C** stretching), 981.72, 1413.73 (**C** (**=O**)-**O-H** bend), 814.90 (**=C-H** bend), 1209.54 (**-C(=O)-O** stretching), 1162.15 (**-C(=O)-O** stretching), 981.72 (**=C-H** bend).

3.4. Self-Crosslinking of ESOCOMA network (5)

The ESO-COMA network polymer was prepared with the stoichiometry given above. 1-2% (wt) dicumenyl peroxide (based on the mixture) and small amount of CH_2Cl_2 to facilitate mixing were added to the mixture and well stirred. The mixture is transferred to a Teflon mold and CH_2Cl_2 was evaporated. The mold was heated at 80°C for 4 hrs and then at 150 °C for 2 hrs. The thermoset obtained has a darker shade of yellow than the ESO-COMA adducts and has higher toughness.

IR Spectrum (cm^{-1}): 3467.92 (**O-H**), 2925.51, 2854.83, and 1459.72 (**C** (sp^3)-**H** stretching), 1735.66 (**C=O** stretching), 1641.98 (**-C=C** stretching), 1162.31 (**-C(=O)-O** stretching)

3.5. Simultaneous Interpenetrating Polymer Networks with ESOCOMA

3.5.1. ESOCOMA-St Network (6)

The ESO-COMA-Styrene mixtures were prepared at different weight ratios, benzoyl peroxide (1% wt) as free radical initiator was added and the mixture was transferred into Teflon mold. The mixture was kept at 70-80 °C for overnight. The resultant network polymer has a lighter yellow shade and is more brittle than the ESO-COMA adduct. The characterization was carried out via IR analysis. The sample is insoluble in organic solvents.

IR Spectrum (cm^{-1}): 3468.8 (**O-H**), 2924.0, 2854.2, and 1455.5 (C (sp^3)-H stretching), 1737.6 (**C=O** stretching), 1644.7 (-C=C stretching), 1209.1 (C-C (=O)-**O** stretching), 980.2 (=C-**H** bend), 724.0, 699.8 (=C-**H** bend, aromatic ring).

3.5.2. ESO-COMA-AESO Network (8)

The ring opening reaction between ESO-COMA and the reactions of unsaturated C=C double bonds on COMA(2) and AESO (7) via free radical mechanism were carried out simultaneously. The ESO-COMA-AESO mixtures were prepared at different weight ratios, benzoyl peroxide (1% wt) as free radical initiator was added to the mixture and transferred into Teflon mold. The mixture was kept at 70-80 °C for overnight. The resultant network polymer has a darker yellow shade. The characterization was carried out via IR analysis.

IR Spectrum (cm^{-1}): 3435.9 (**O-H**), 2924.0, 2854.1, and 1455.9 (C (sp^3)-H stretching), 1731.1 (**C=O** stretching), 1644.7 (-C=C stretching), 1209.4 (C-C (=O)-**O** stretching).

4. RESULTS AND DISCUSSION

The first step of the project was the maleation of castor oil which gives the maleated half ester (COMA, 2). The second step was the formation of a thermoset (ESOCOMA, 3) by using COMA as the epoxy curing agent for another oil based monomer ESO. In the third step ESOCOMA, which still carries an intact unsaturation on maleate group, was used to give a second network (Styrene-X, 6), with styrene as the reactive diluent. The two networks are thus interpenetrating. As a separate approach, instead of styrene one other oil based macro-monomer, AESO (7) was also used to form the second network via free radical reaction between maleate and acrylate groups to give another interpenetrating network (AESO-X, 8). In this network the epoxy component (ESO), the epoxy curing agent (COMA) and the reactive diluent (AESO) are all plant oil-based. The characterization of those products was done by IR spectroscopy, thermal and mechanical tests such as DSC (Differential Scanning Calorimetry), DMA (Dynamic Mechanical Analysis).

4.1. Characterization of COMA (2)

Synthesis of COMA has been described in the literature (20). In this project COMA synthesis was modified to increase the maleate content of the product. Castor oil/ maleate ratio in the feed was increased to 3 and a reaction time of 7-8 days and reaction temperature of 90-100 °C was chosen.

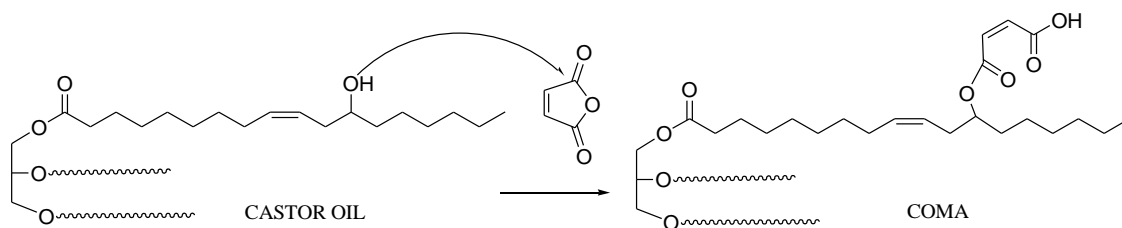


Figure 4.1. Maleation of Castor Oil.

The product has a darker yellow shade and higher viscosity than castor oil and is soluble in common organic solvents such as acetone, toluene, THF, CH_2Cl_2 . The characterization was carried out via IR and NMR analysis.

4.1.1. Spectral Identification

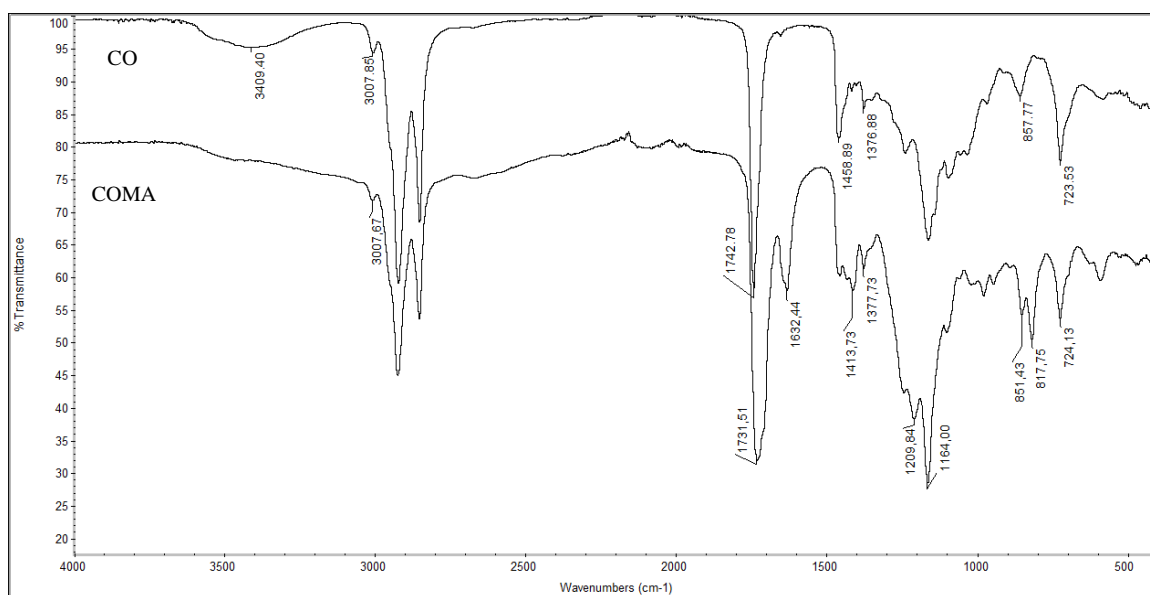


Figure 4.2. IR Spectra of Castor Oil (1) and Maleated Castor Oil (2).

The IR spectrums of castor oil (CO) and COMA is given above. The peak at 3409 which corresponds to hydroxyl stretch is observed to disappear, to be replaced by the broad carboxylic acid peak. After maleation, two kinds of carbonyl groups are formed, one is the α - β unsaturated ester and the other is the α - β unsaturated carboxylic acid. Considering also the carbonyl groups of the triglyceride esters, the broad peak at 1732 could be identified as the overlap of all those different carbonyl absorptions. Identification of those separate carbonyls is not possible, yet the location of the peak is shifted from 1742 to 1732 exhibiting the effect of both α - β unsaturation and carboxylic acid group. The increase in the intensity of the peak at 1632 and the new peak at 817 are due to the stretching motion of sp^2 hybridized carbon atoms on maleate group and ($=\text{C-H}$) bending motions, respectively. Finally, the peak appearing after maleation at 1413 could be attributed to the bending motion of hydroxyl group of the carboxylic acid.

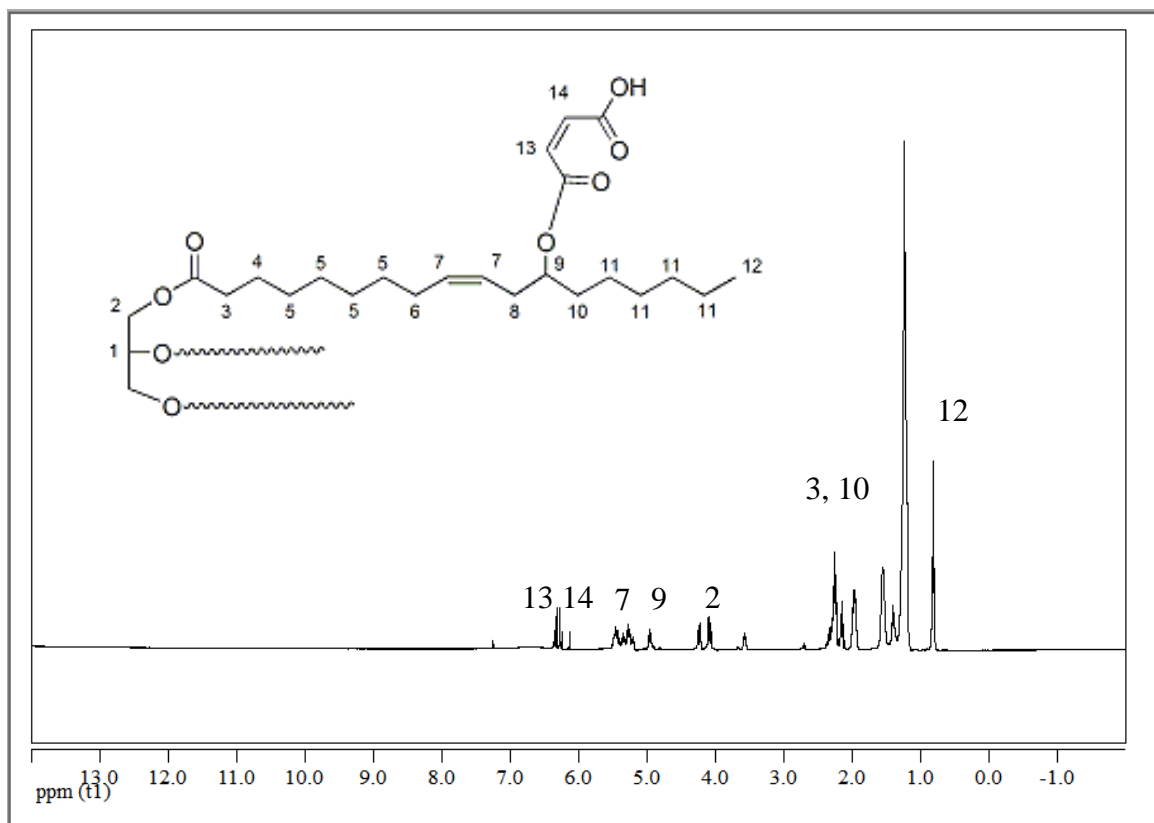


Figure 4.3. ^1H - NMR spectrum of COMA (2).

In the ^1H - NMR spectrum of COMA (Figure 4.3), the peak number 12 is the methyl group appearing as a singlet at 0.9δ . The small peak at 3.6 indicates the presence of unreacted hydroxyl group, however in a very low amount. The glycerol protons appear at 4.1δ , labeled as 2 in figure. The peak at 5.0δ labeled as 9 shows the proton of the carbon atom attached to maleate. There are two different types of vinyl protons in the molecule. The peaks at 5.2 - 5.6δ are the protons of the vinyl group on fatty acid chain, whereas the peaks at 6.4δ indicate the vinyl group on maleate. The isomerization of maleate to fumarate occurs due to prolonged heating and the peaks at 6.1δ represent the vinyl protons of fumarate. The very small peak at 7.1δ is assigned to the unreacted maleic anhydride. Maleic anhydride sublimes easily; therefore the absence of maleic anhydride in the product cannot be taken as complete consumption of maleic anhydride.

4.1.2. Determination of Maleation Ratio by NMR Spectrum

The maleation ratio of COMA was calculated using the NMR peak integrations. The peaks corresponding to terminal protons at CH_3 at the end of fatty acid and vinyl protons on the maleate were compared. The maleation number is deduced from this ratio. The methyl protons appear at 0.9 as singlet and vinyl protons appear at 6.1- 6.4 as multiplets, the ones at 6.1 belonging to fumarate isomer.

In castor oil, there are 9 CH_3 protons and on average 2.44 -OH groups to be maleated (20). If all hydroxyl groups were maleated, 4.88 vinyl protons would be observed in the spectrum. Thus the theoretical ratio of vinyl protons to methyl protons in a fully maleated molecule is 0.54. The integrals obtained from spectra are 2.4 to 1 for methyl and vinyl protons respectively resulting in a ratio of 0.41. The maleation percentage is calculated to be 75%, giving a 1.83 moles of maleate per triglyceride. Attempts to increase the maleation ratio resulted in a product that was too viscous and were abandoned.

The hydroxyl group of castor oil is a secondary alcohol and is capable of undergoing esterification reaction with maleic anhydride. Considering the fact that being a secondary alcohol, the reactivity of hydroxyl group will not be high, the reaction time was extended to 3-5 days for higher maleation ratio. Also, by heating the product at 60 °C for 2-3 days, the yield was increased. In order to shorten those long periods of reaction time, which is not desirable in industrial production, utilization of catalysts could be considered.

One other disadvantage of the synthesis is the necessity of using a solvent in order to prevent the sublimation of maleic anhydride. The solvent should have a high boiling point so as to carry out the reaction at high temperature, yet not so high that the removal after reaction is difficult. In this case, the solvent was selected as toluene. The removal of the solvent was carried out under vacuum at 60 °C along with the removal of un-reacted maleic anhydride.

Castor oil has a lighter shade of yellow, but after maleation the color darkens and the viscosity increases. The characterization was carried out with IR and H-NMR spectra. The maleation number was determined as 1.8 per triglyceride from NMR integration.

According to the NMR spectrum, 75% of the hydroxyl groups in the castor oil were maleated.

4.2. Characterization of ESOCOMA (4)

ESO is industrially synthesized by epoxidation of soybean oil having an Iodine number of 145 with performic acid. The epoxidation extent of the commercial ESO used in this work, given by the manufacturer, was 4.2 epoxy groups per triglyceride. This was previously determined in our lab by HI titration and was found to be correct.

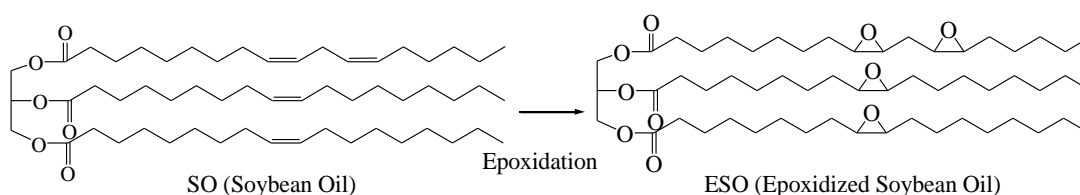


Figure 4.4. Epoxidation of Soybean Oil.

The extent of maleation of COMA previously described gives 1.8 maleates per triglyceride. Stoichiometry of the reaction was chosen based on these numbers. With this knowledge the ideal mole ratio of COMA/ESO has been found to be 2.3, which gives the ideal mole ratio of reacting groups.

The constraints such as reduction in diffusion rates and immobility due to high molecular weights obtained as the reaction proceeds are not considered here. It is also probable that the alkoxide formed after ring opening of the epoxide may open another epoxide leading to epoxide homopolymerization. This, of course consumes epoxide groups. Therefore, it is impossible to determine a theoretical stoichiometry and the experiments with different ratios will be required. In this work, several mol ratios close to the calculated ratio were tried. When the ratio of COMA to ESO is increased above 2.0, the adduct turns out to be a sticky, and tacky gel-like material. Taking the ratio 2 as the top limit, several trials were conducted and the compositions are given below in a tabulated form together with the surface hardness values measured with Zwick/Roell Durometer.

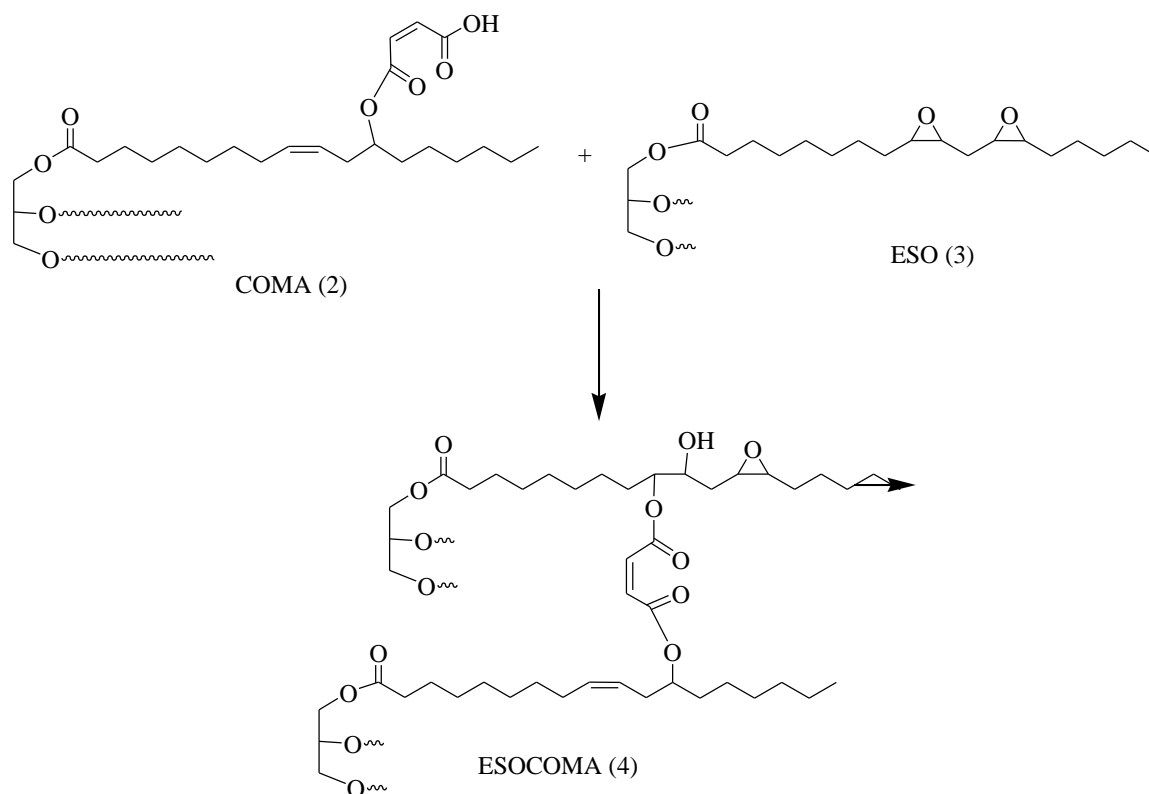


Figure 4.5. Reaction of COMA with ESO.

Table 4.1. Surface Hardness Values for Optimization of COMA/ESO Ratio.

Run	1	2	3	4	5	6
COMA/ESO	0.47	0.67	1.44	1.50	1.68	2.00
Hardness	26	26	45	52	45	42

Surface hardness was chosen as a quick and efficient way of evaluating samples. Based on the surface hardness values the optimum mole ratio was determined to be 1.5. Yet, even with the optimized quantities, adduct is very flexible and soft at room temperature.

4.2.1. Spectral Identification of ESOCOMA (4)

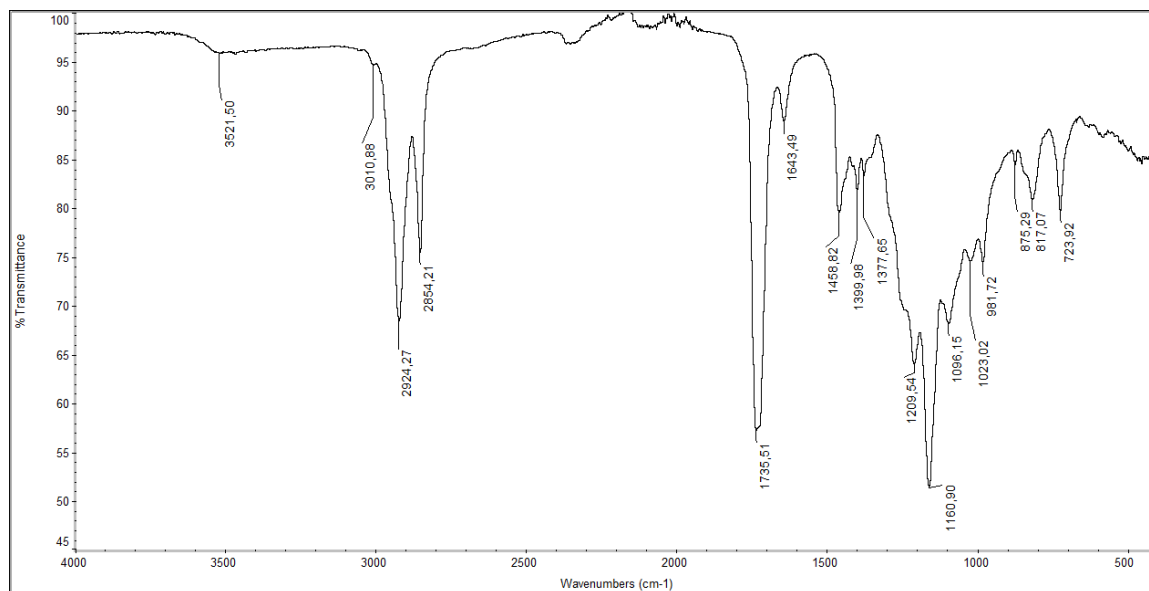


Figure 4.6. IR Spectrum of ESOCOMA.

The peak at 3521 corresponds to hydroxyl groups created by the opening of epoxy rings. The peak at 1413 and 978 has disappeared indicating the consumption of carboxylic acid ends of COMA. The broad $-OH$ peak centered around 3200 has disappeared indicating the consumption of free $-COOH$ groups. There are several carbonyl groups in adduct, they all overlap and cannot be distinguished. At the end of the reaction, the peak at 1731 shifted to 1735, which is a very minor change considering the fact that the ester peak of ESO is not much different than the COMA ester peaks. In addition, there are no peaks around 830 corresponding to oxirane ring, which indicates that there are no epoxy rings left unreacted. As COMA is a highly crosslinked thermoset polymer, it is not soluble in common NMR solvents and no NMR spectrum can be obtained.

4.2.2. Thermal and Mechanical Properties of ESOCOMA (4)

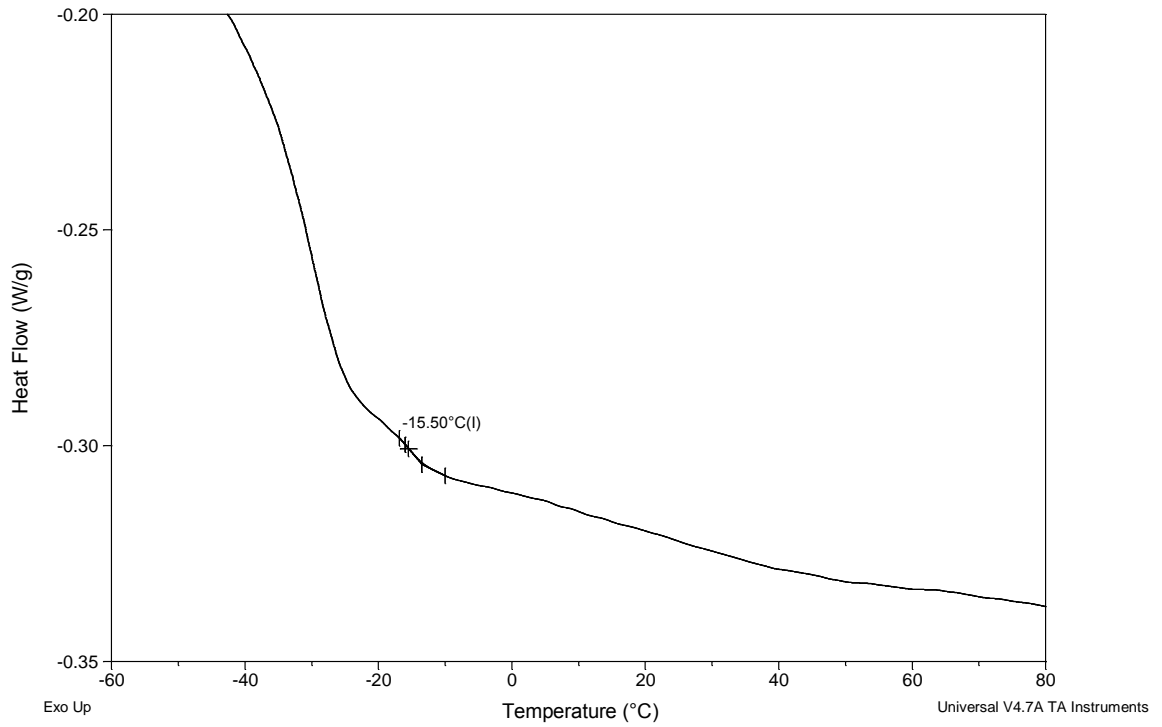


Figure 4.7. DSC Analysis graph of ESOCOMA (4).

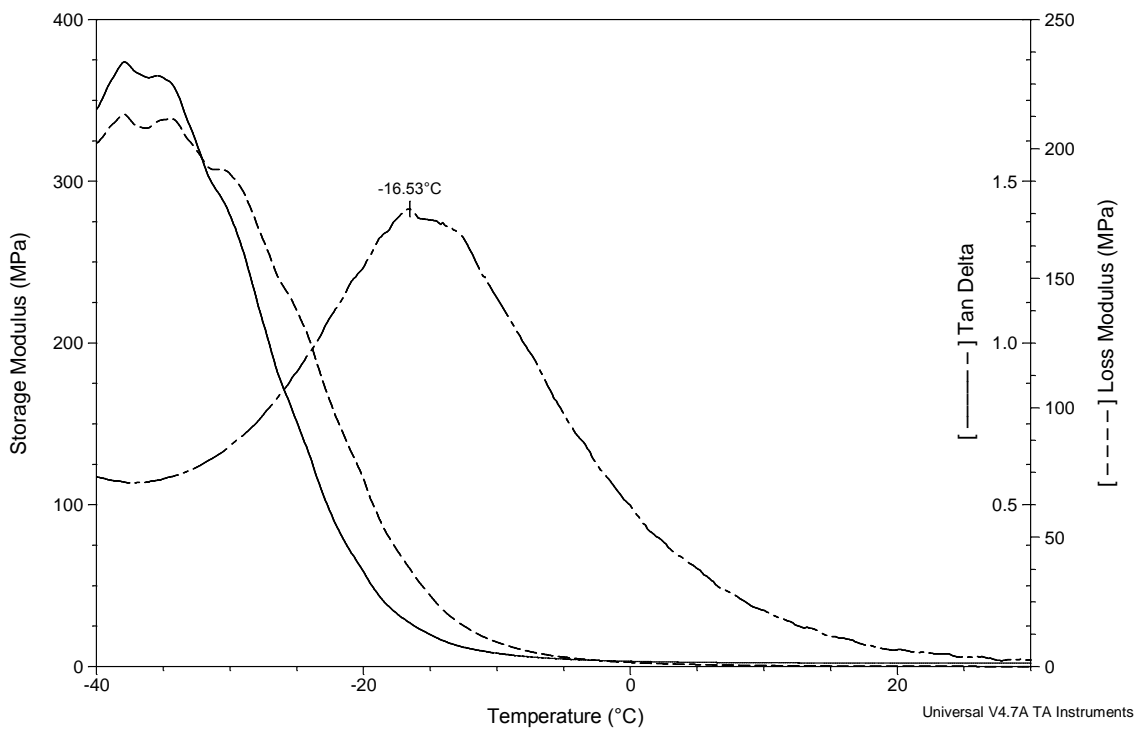


Figure 4.8. DMA Graph of ESOCOMA (4).

DSC analysis shows a glass transition temperature of $-15.50\text{ }^{\circ}\text{C}$, which is an expected result because of the free motion of large triglyceride alkyl chains and the absence of a rigid component in the polymer. The change in slope is not observed very clearly in DSC graph, yet the value obtained from DMA is $-16.53\text{ }^{\circ}\text{C}$, which is close to DSC result. Since the change in slope of the curve is not very distinct in the graph, it is safer to take the DMA result as the correct data for T_g . The storage modulus of adduct at room temperature is determined as 2.1 MPa and the storage modulus at a temperature $30\text{ }^{\circ}\text{C}$ above the T_g is found as 2.38 MPa, which shows the low mechanical strength of the adduct.

4.3. Characterization of self-crosslinked ESOCOMA (selfX) (5)

4.3.1. Spectral Identification of selfX (5)

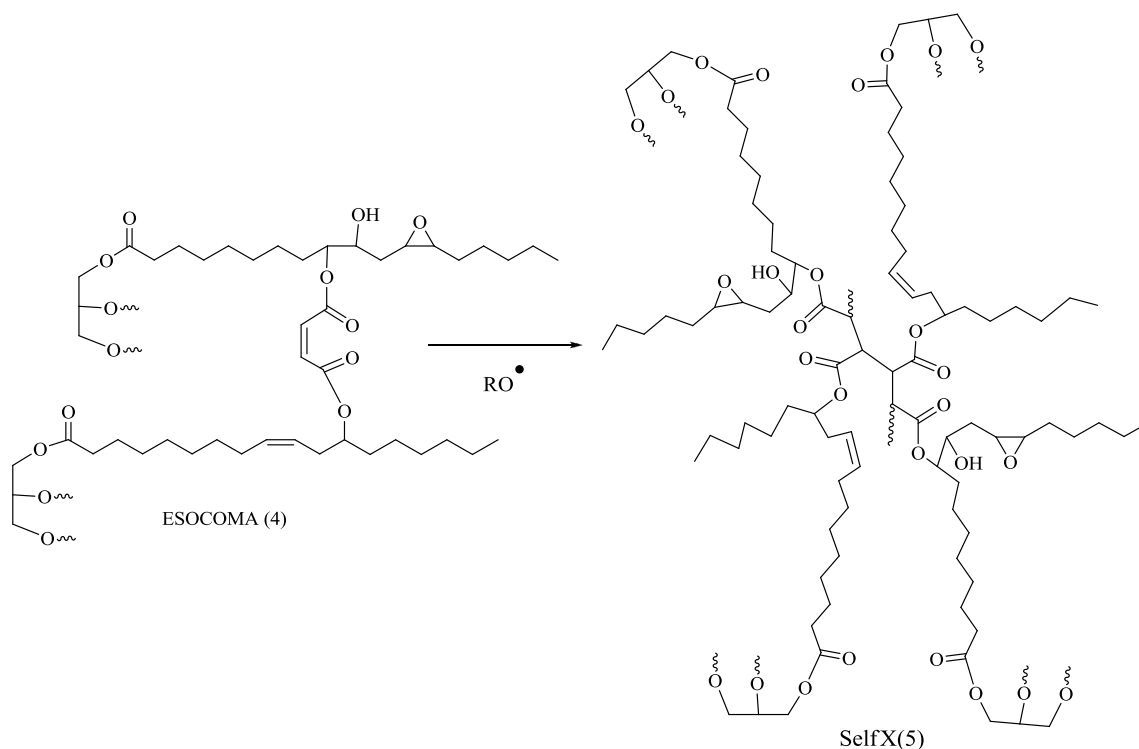


Figure 4.9. Self Crosslinking reaction of ESOCOMA.

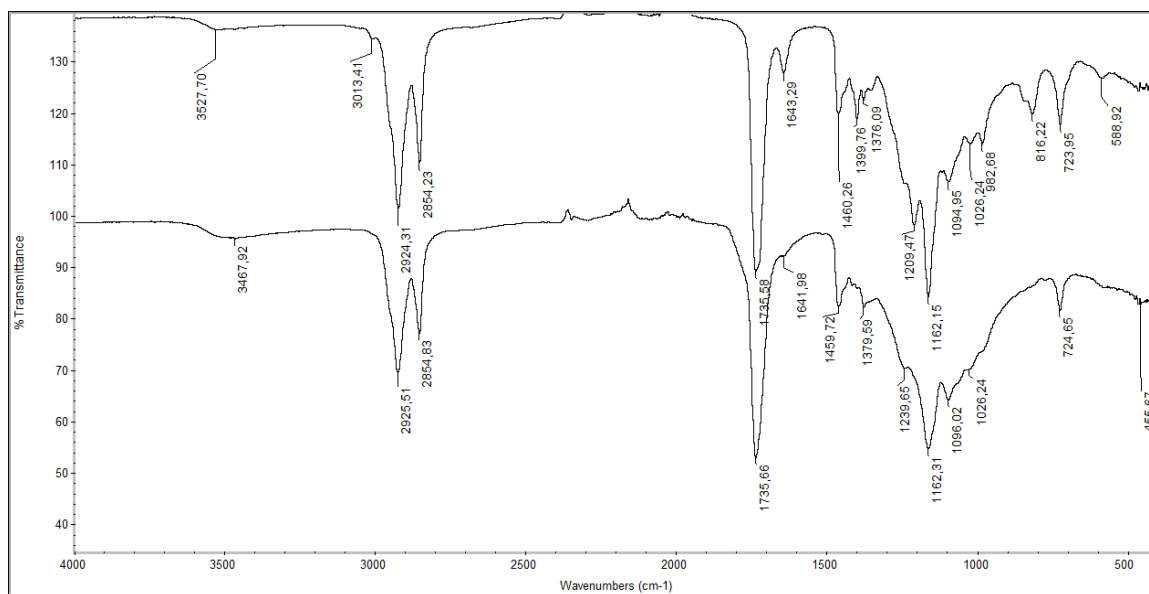


Figure 4.10. IR spectra of SelfX, pre and post reaction.

While ESOCOMA adduct is a crosslinked material due to ring opening reaction of the carboxylic acid groups with epoxides, the maleate double bonds and the triglyceride double bonds are still intact. Double bonds on the maleate groups and on the fatty acid chain of the ricinoleic acid residues were polymerized free radically. When functional groups that need to react (in this case double bonds) are part of a crosslinked network, serious diffusion problems arise and migration of the double bonds to within reaction distance is expected to be very difficult. Surprisingly, the highly reactive maleate double bonds and the comparably unreactive triglyceride double bonds reacted almost completely with each other. The extent of the reaction could be followed by observing the peaks due to sp^2 hybridized carbons. In the spectra given above, the peaks at 3013 corresponding to $C=C-H$ stretches, and at 814 and 981 corresponding to $=C-H$ bend disappeared. The peak at 1643, corresponding to $-C=C$ stretching decreased in intensity. Since self crosslinking only occurs at unsaturated sites, there are no changes on the other sites of the molecule, thus no other changes in the spectra before and after the reaction were observed. The most tangible evidence for the reaction is a dramatic increase in the mechanical properties of the polymer upon increase in connectivity.

4.3.2. Thermal and Mechanical Properties of selfX (5)

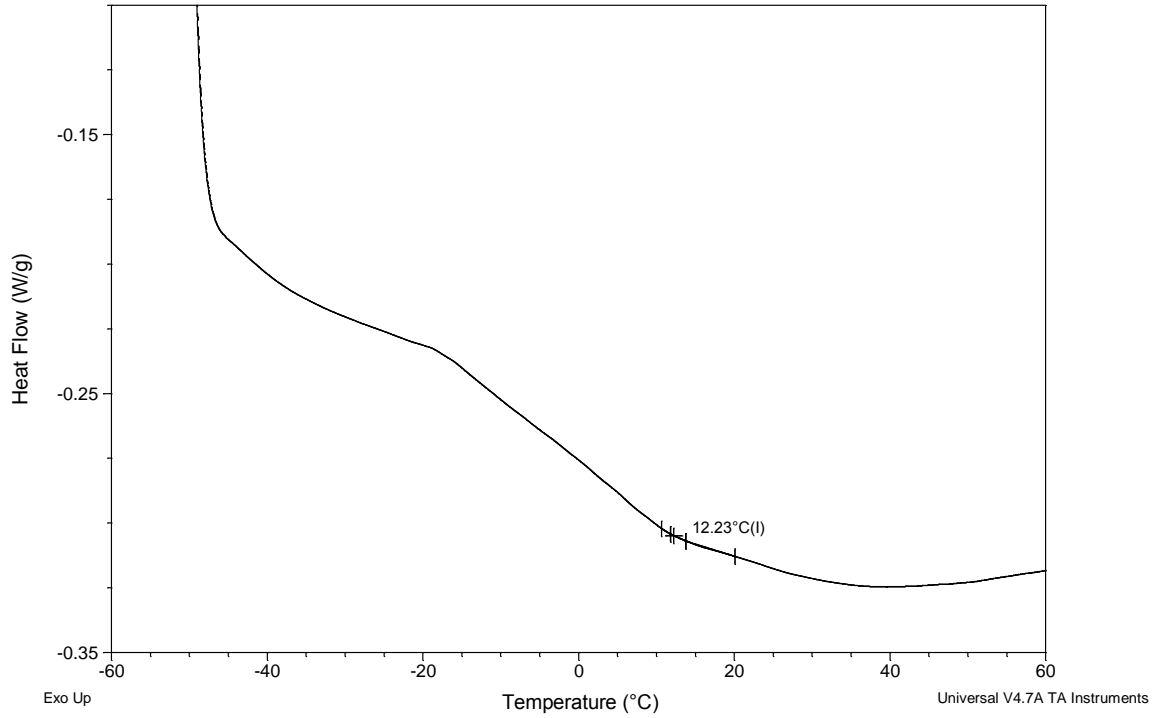


Figure 4.11. DSC Analysis graph of selfX(5).

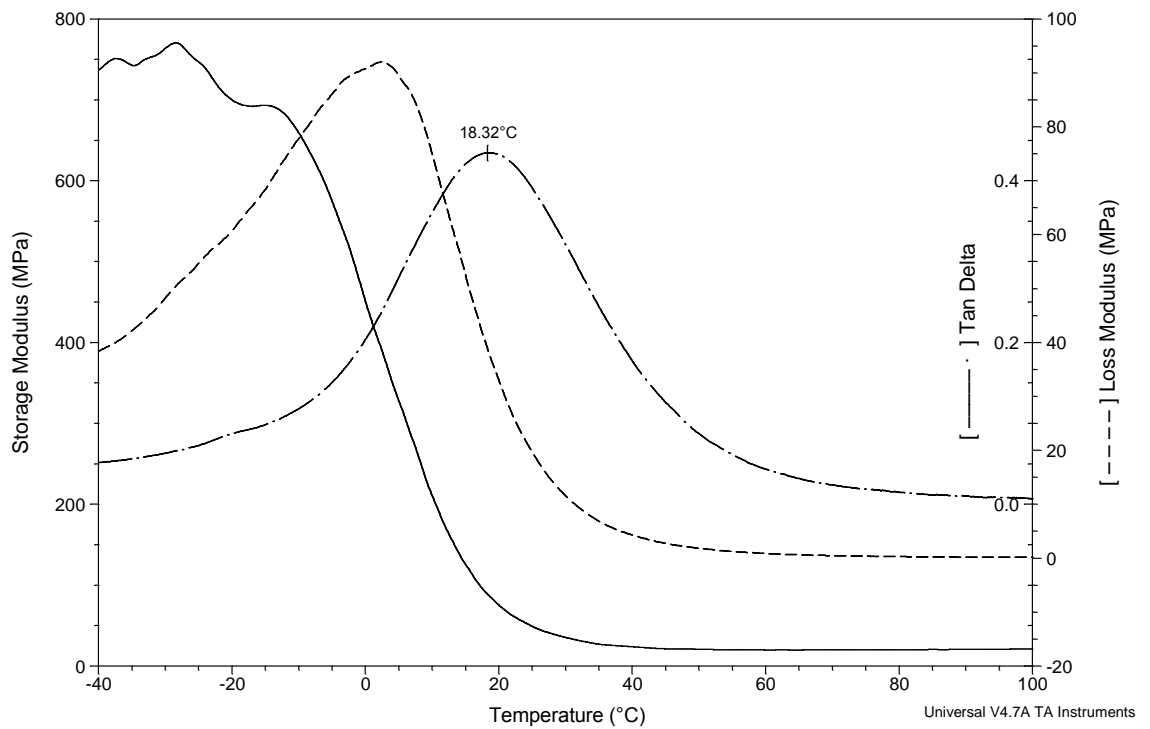


Figure 4.12. DMA Graph of selfX(5).

DSC plot for selfX shows a glass transition temperature of 12.23 °C which is still below room temperature, yet much higher than ESOCOMA. The result of the DSC differs from the DMA data by 8 °C, and it is safer to take DMA data as the correct one, since the change in slope in DSC graph is not very distinct. According to DMA data, the glass transition temperature is 18.62 °C, which is 34 °C, higher than ESOCOMA. Such an increase in T_g shows the decrease in the flexibility of the long alkyl chains. With the reaction of maleate double bonds, the crosslinking density is increased giving rise to a more rigid material, the increase in mechanical properties with increased connectivity is also observed in storage modulus values as well. As given in Table 4.2, the storage modulus for selfX at room temperature increased up to 25 times of the value obtained before crosslinking.

Table 4.2. Result of mechanical analysis for selfX (5).

	T_g (°C)	Storage Modulus (MPa)*	Storage Modulus at 25 °C (MPa)
ESOCOMA (4)	-16.5	5.1	2.1
SelfX (5)	18.3	566.4	49.0

* The average storage modulus at [-10-0] °C.

4.4. Characterization of Simultaneous Interpenetrating Network of Styrene-X (6)

As the reactive diluent, styrene was introduced to the system. The compositions of the samples are given below in Table 4.3. and Table 4.4. The first number in the sample name stands for the COMA/ESO by weight whereas the second number stands for the styrene's weight percent. Thus in sample Styrene-X 1.5 : 0.25, COMA/ESO ratio by weight is 1.5 whereas the styrene content is 25% of the weight of the sample.

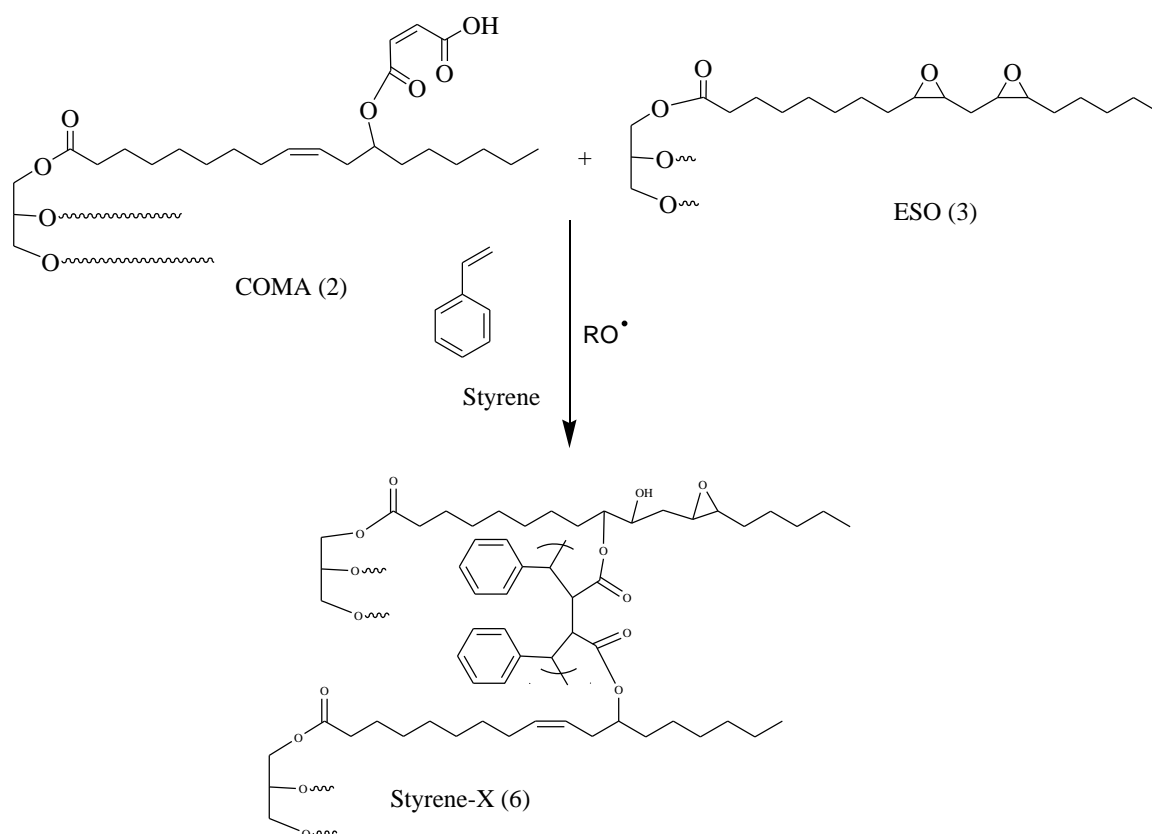


Figure 4.13. Synthesis of Simultaneous IPN of ESO-COMA-Styrene.

Table 4.3. Composition of Styrene-X Network-Constant weight % styrene.

Run	Styrene-X 1.5 : 0.25	Styrene-X 2.0 : 0.25	Styrene-X 2.50 : 0.25	Styrene-X 3.0 : 0.25
COMA/ESO	1.49	2.00	2.50	3.00
wt % Styrene	0.25	0.25	0.25	0.25

Table 4.4. Composition of Styrene-X Network-Constant ratio for COMA/ESO.

Run	Styrene-X 1.5 : 0.10	Styrene-X 1.5 : 0.20	Styrene-X 1.5 : 0.30
COMA/ESO	1.50	1.50	1.50
wt % Styrene	0.10	0.20	0.30

The restricted diffusion of the double bonds of ESOCOMA to each other was mentioned earlier. These problems are traditionally solved by swelling the initial network in a reactive diluent. The reactive diluent is a small polymerizable monomer which will swell the initial network and will freely diffuse due to its low molecular weight. When treated with a free radical initiator, the reactive diluent and the polymerizable groups in the initial network (maleate double bonds in this case) will polymerize into a second and interpenetrating network. Creation of the first network, swelling with a reactive diluent and formation of the second network is best done sequentially. However in this work it was impossible to swell the initial ESOCOMA network in any of the monomers tried homogeneously. The connectivity of the ESOCOMA network was so low that all of the monomers used, including styrene, methyl methacrylate and butyl acrylate fragmented the sample seriously. Decreasing the reactive diluent amount only gave non-homogeneous partially swollen samples. Therefore the traditional sequential interpenetrating network formation could not be carried out.

Instead, ESOCOMA reaction was run in styrene solvent so as to give the initial ESOCOMA network already swollen in styrene. This was simultaneously free radically polymerized and therefore this product is called simultaneous interpenetrating network of ESOCOMA with styrene. At the reaction temperature both epoxide ring opening polymerization with carboxylate and the double bond copolymerization of styrene with maleate are quite fast and it was impossible to determine which preceded which. Regardless, when the final product was post cured no loss of weight was observed indicating that all of styrene was incorporated into the second network.

4.4.1. Spectral Identification

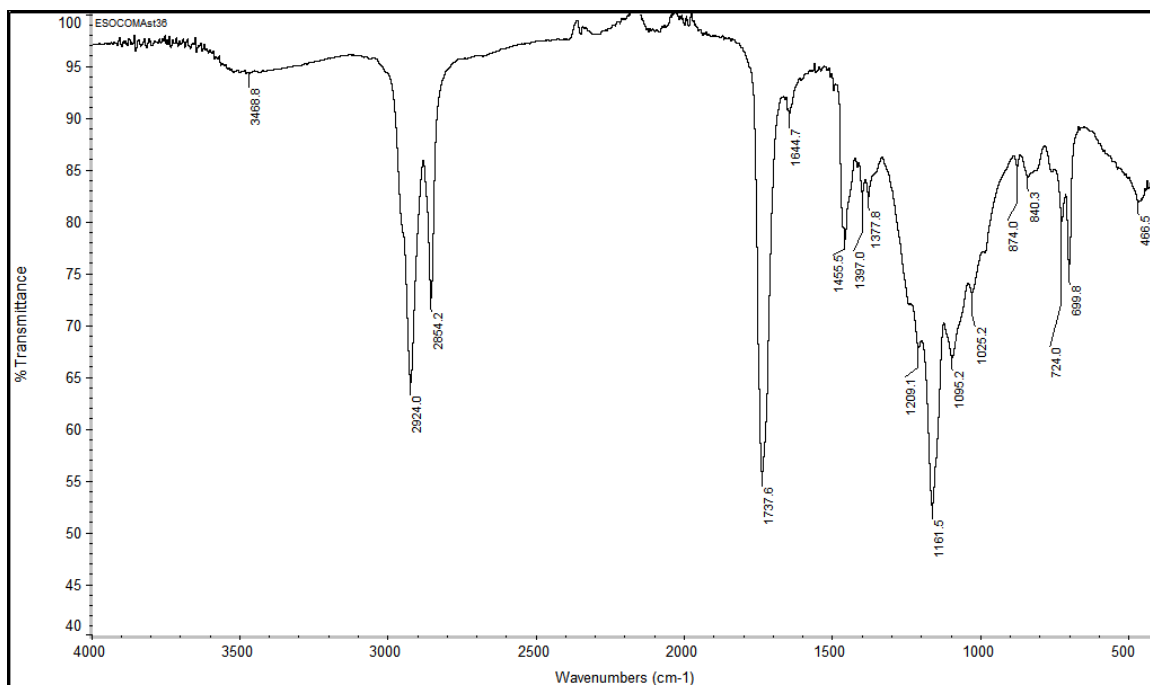


Figure 4.14. IR Spectrum of Styrene-X Network (6).

As the interpenetrating network is insoluble, IR was the only available analytical tool. The peak at 3468 corresponds to hydroxyl end of opened epoxy rings. The disappearing of the peaks at 3200, 1413 and 978 indicates the consumption of carboxylic acid ends of COMA. The peak just above 3000, indicating the vinyl protons of the maleate and styrene have disappeared since those vinyl groups are consumed at the end of the free radical reaction. The aromatic stretching vibrations of styrene, which should have appeared above 3000 are not observed in the spectrum since the amount of styrene in adduct is very small. The peaks at 724 and 699 are assigned as the bending motion of aromatic ring hydrogens.

4.4.2. Mechanical Properties

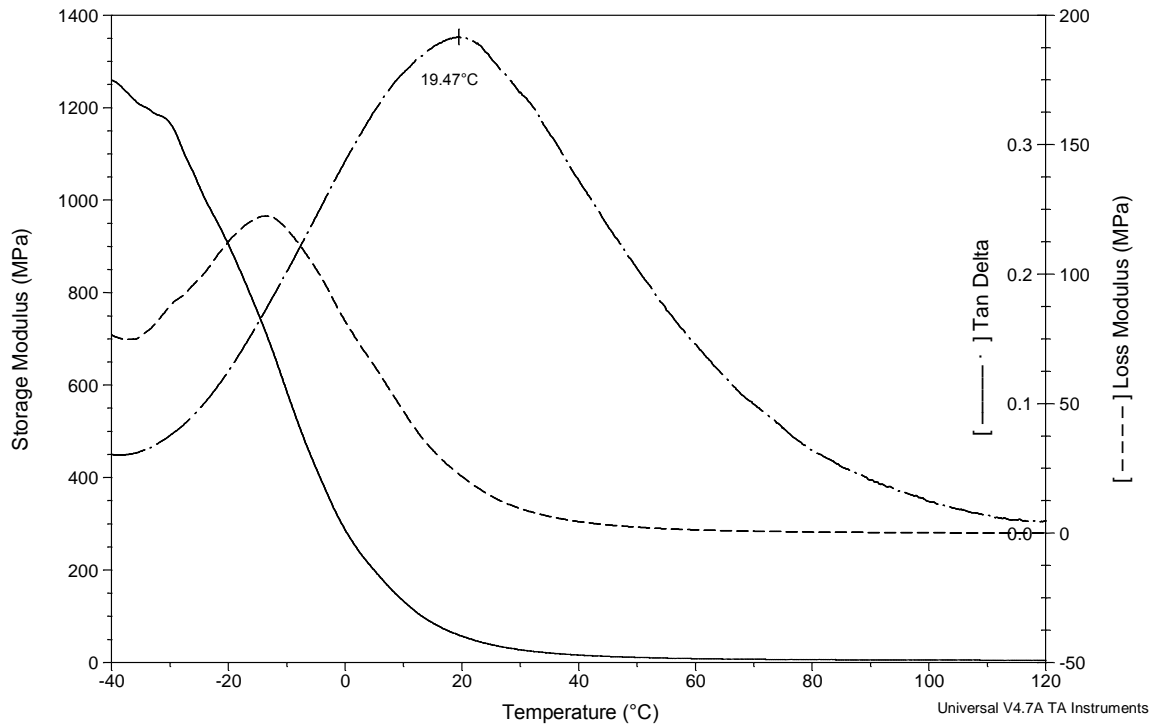


Figure 4.15. DMA Graph of Styrene-X 1.5 : 0.25.

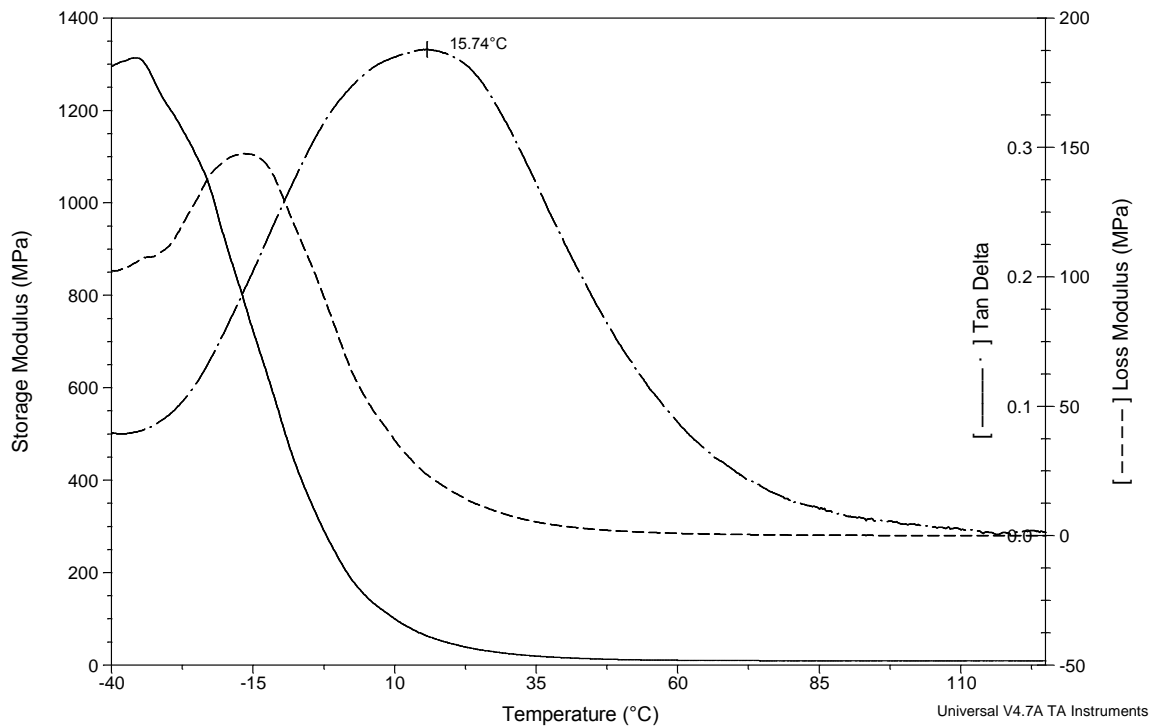


Figure 4.16. DMA Graph of Styrene-X 2.0 : 0.25.

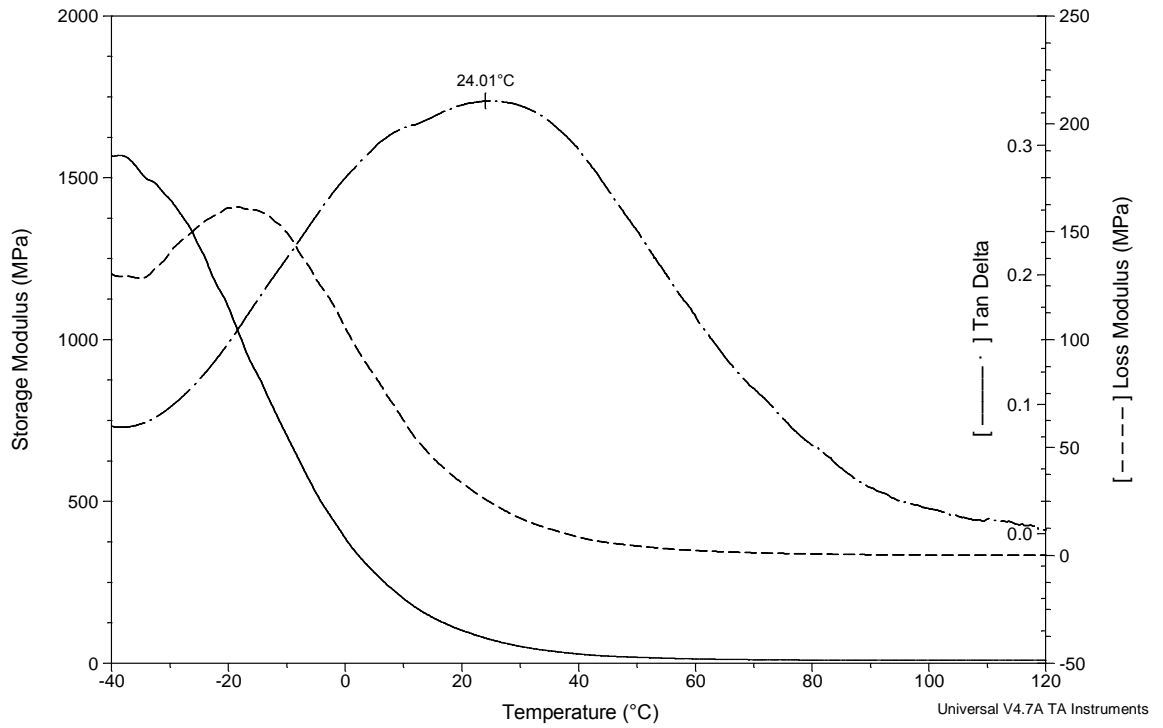


Figure 4.17. DMA Graph of Styrene-X 2.5 : 0.25.

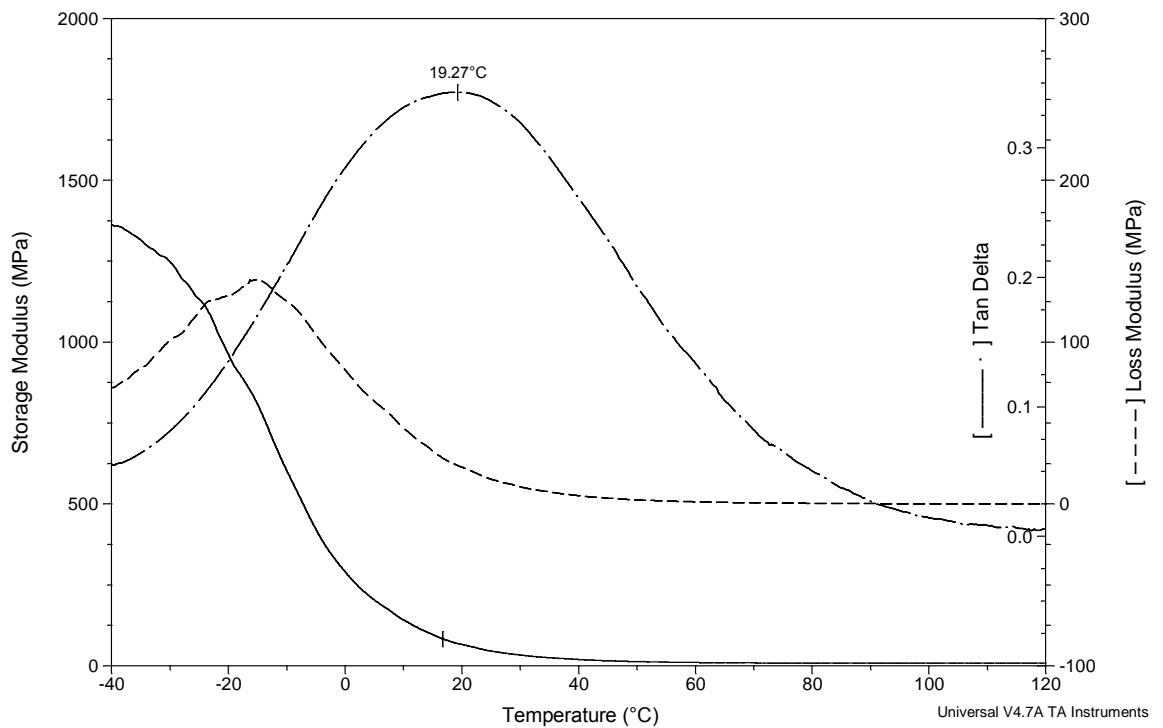


Figure 4.18. DMA Graph of Styrene-X 3.0 : 0.25.

Samples were made where COMA:ESO ratio were varied but the overall styrene content was kept constant. The effect of COMA:ESO ratio of the initial network on the properties of the final network at constant styrene ratio was examined and the results are shown in Table 4.5.

DMA graphs of Styrene-X adducts show T_g values varying from 19.5, 15.7, 24.0, 19.3 °C with increasing COMA content of the initial network. As could be seen from Table 4.6, compared to ESOCOMA, the T_g values and the storage modulus values increased upon formation of the second network. The increase is both due to the presence of rigid styrene units and the increase in crosslinking densities. Upon addition of styrene to the network, the best mechanical properties are observed when the ratio of COMA to ESO is 2.5. This ratio is different than the value obtained by the surface hardness results of ESOCOMA adducts which does not include styrene. Such a difference is not unexpected since the number of molecules that may react with COMA increased with the addition of styrene as well as the increased mobility of reactants with reactive diluent styrene, thus overcoming the diffusion limitation. In other words, addition of styrene introduces another functionality to the network which will tie COMA to other components, and prevent the softening effect of the unreacted COMA molecules. However, the increase in COMA amount is compensated only up to a certain extent and further increase in COMA does affect the mechanical property inversely, possibly owing to the decrease in ester linkage of ESO and COMA due to insufficient ESO amount.

As expected, the DMA analyses show an increase in T_g and storage modulus with increasing styrene content. The sample Styrene-X 1.5 : 0.25 from the first set also fit into that trend. Considering the styrene composition of sample Styrene-X 1.5 : 0.25 corresponds to a point between Styrene-X 1.5 : 0.20 and Styrene-X 1.5 : 0.30, the T_g value should be between 12.30 and 25.78, and this is found to be the case. One could conclude that the increase in styrene composition increases the glass transition temperature.

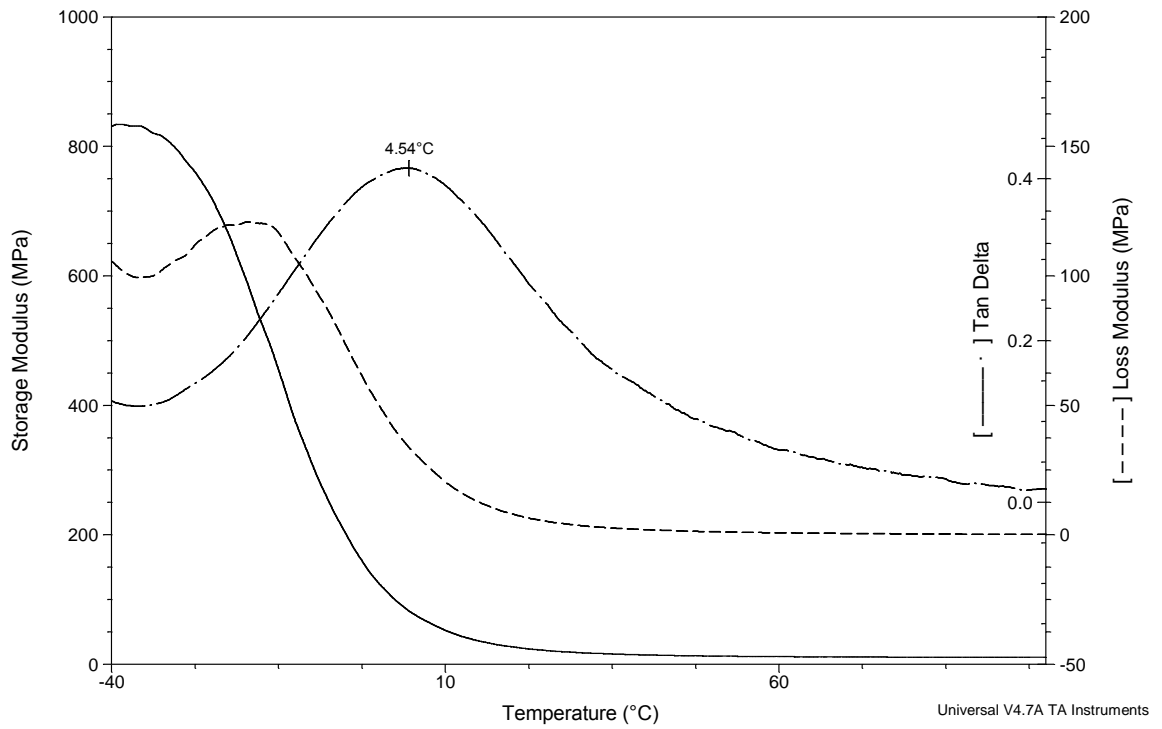


Figure 4.19. DMA Graph of Styrene-X 1.5 : 0.10.

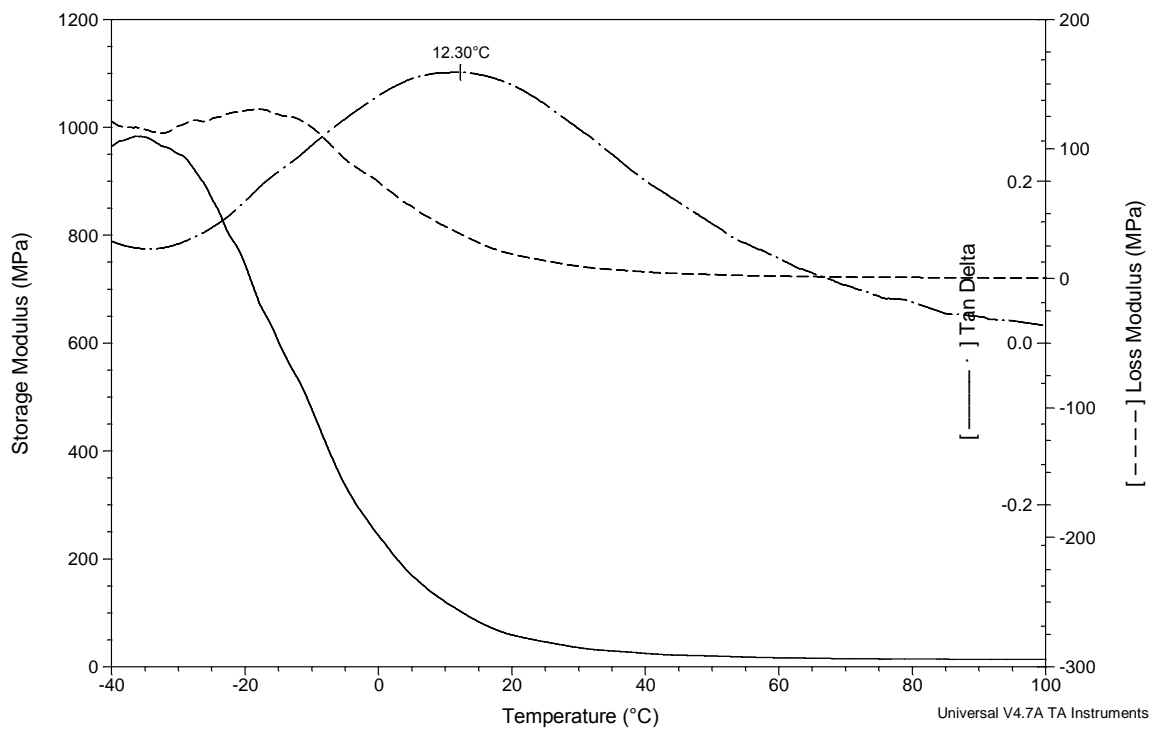


Figure 4.20. DMA Graph of Styrene-X 1.5 : 0.20.

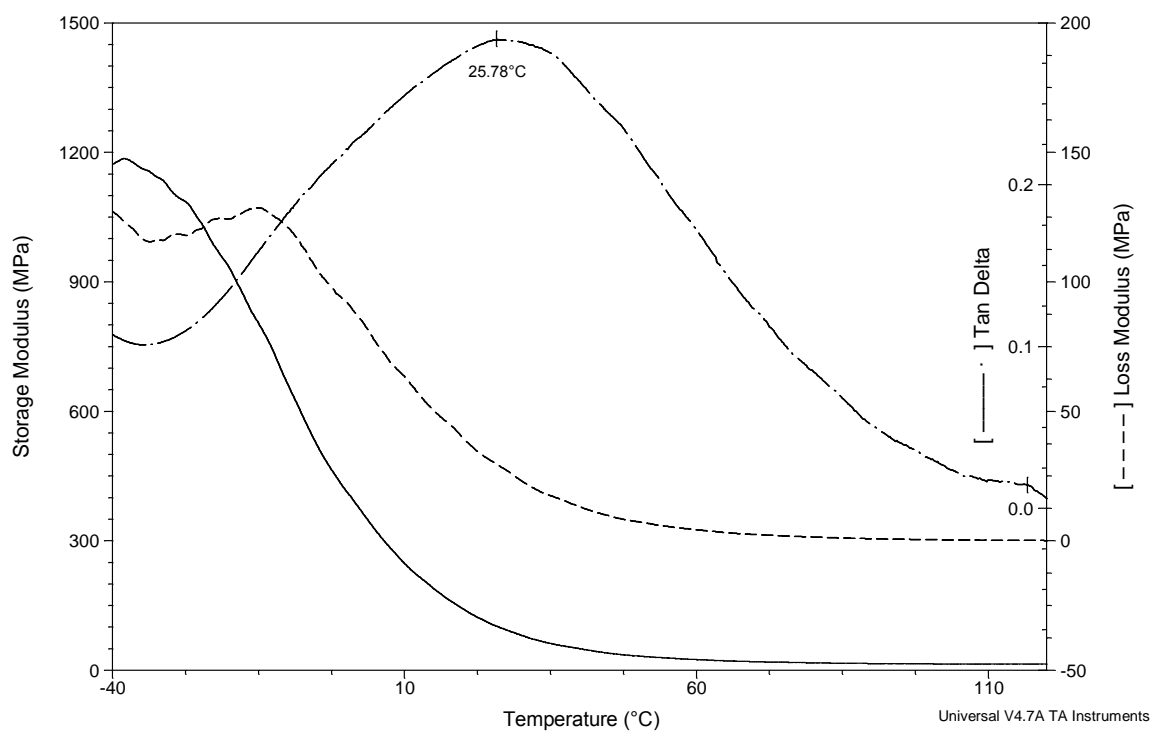


Figure 4.21. DMA Graph of Styrene-X 1.5 : 0.30.

Table 4.5. Result of mechanical analysis for Styrene-X (6) Adducts.

	T_g (°C) DMA	Storage Modulus (MPa)*	Storage Modulus at 25 °C (MPa)
ESOCOMA (4)	-16.5	5.1	2.1
Styrene-X 1.5 : 0.25	19.5	425.2	38.8
Styrene-X 2.0 : 0.25	15.7	365.0	33.2
Styrene-X 2.5 : 0.25	24.0	534.1	72.8
Styrene-X 3.0 : 0.25	19.3	430.9	45.6
Styrene-X 1.5 : 0.10	4.6	207.7	21.5
Styrene-X 1.5 : 0.20	12.3	346.1	46.2
Styrene-X 1.5 : 0.30	25.8	528.5	106.1

* The average storage modulus at [-10-0] °C.

4.5. Characterization of Simultaneous Interpenetrating Network of AESO-X (8)

As the overall aim of this work is to prepare interpenetrating networks with maximum triglyceride content, acrylated epoxidized soybean oil (AESO) was used as the reactive diluent. The synthesis is shown below in Figure 4.22. Actually, AESO is not an ideal reactive diluent as it is quite viscous and has a molecular weight of about 1200 which would hinder its diffusion greatly. Nevertheless, in keeping with the original goals of the project, AESO was used neat and in various solvents as the reactive diluent for ESOCOMA initial network. The ESO-COMA initial network could not be swollen in AESO; even with the aid of a solvent which should provide some mobility to AESO as well as increase the accessibility of ESO-COMA network. AESO could not penetrate into adduct to establish a homogeneity and swollen samples could not be obtained, leaving the previously used simultaneous route as the only option. The same nomenclature is applied here, the first number stands for the COMA/ESO ratio whereas the second number shows the AESO weight fraction in the sample.

When ESO and COMA were reacted in the presence of AESO and the mixture was concurrently treated with a free radical initiator, a simultaneous interpenetrating network was obtained where the acrylate on the AESO reacted readily with the maleate double bonds. In this network, all three components of the final network, namely ESO, COMA and AESO are plant oil triglycerides resulting in a 100% vegetable oil base content.

Table 4.6. Composition of AESO-X Network- Constant ratio for COMA/ESO.

Run	AESO-X 1.5 : 0.15	AESO-X 1.5 : 0.30	AESO-X 1.5 : 0.40
COMA/ESO	1.50	1.50	1.50
wt % AESO	0.15	0.30	0.40

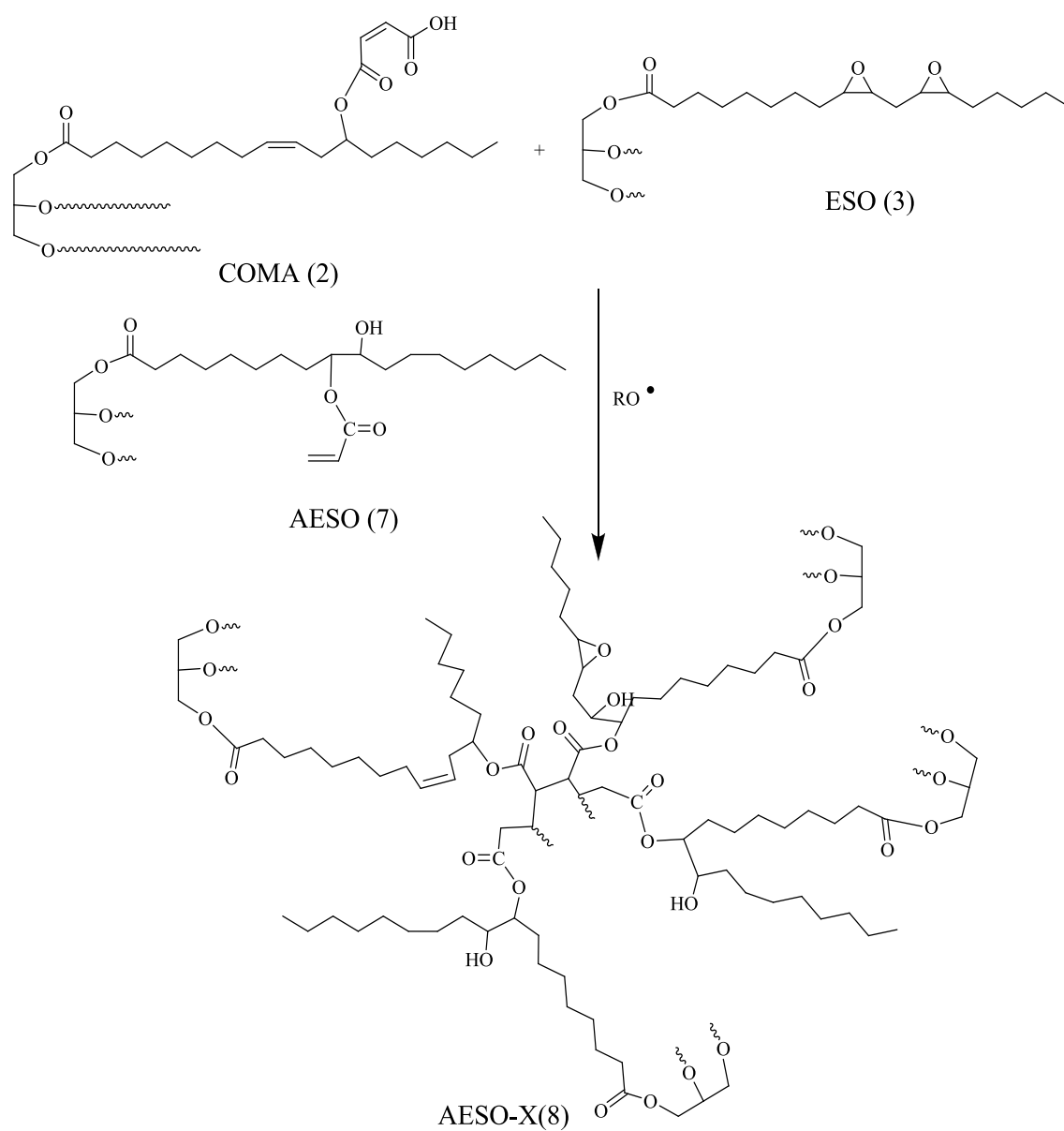


Figure 4.22. Synthesis of simultaneous IPN of ESO-COMA-AESO.

4.5.1. Spectral Identification

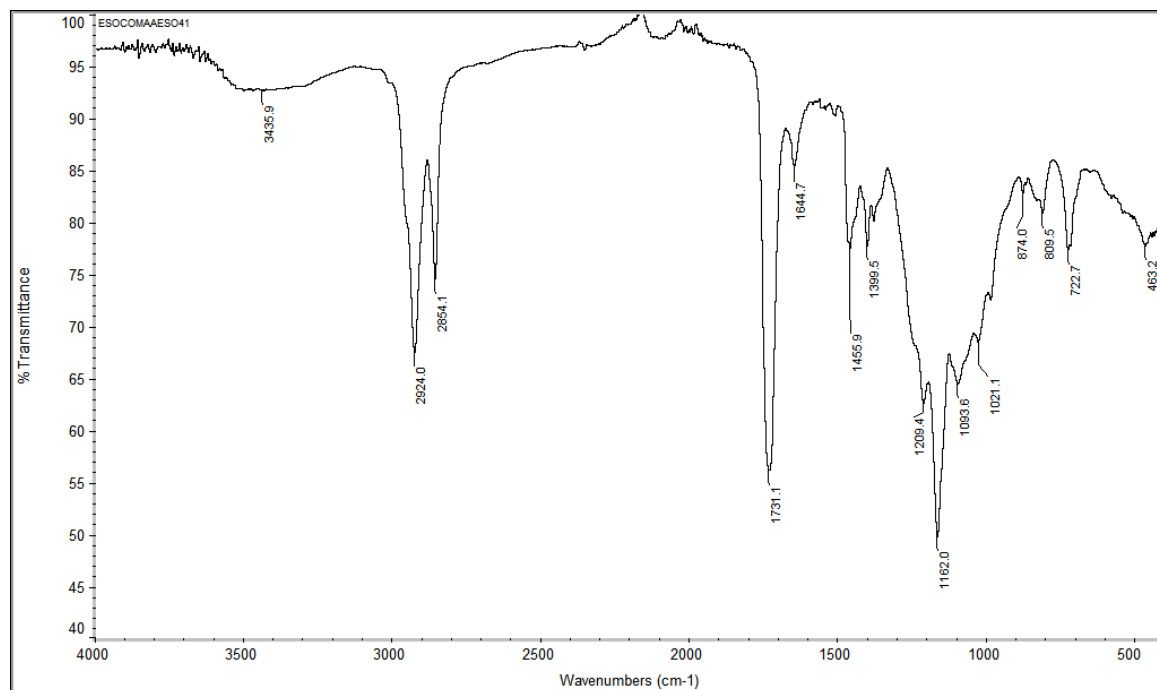


Figure 4.23. IR Spectrum of AESO-X Network.

The peak at 3435 corresponds to hydroxyl end of opened epoxy rings. The disappearing of the peaks at 3200, 1413 and 978 indicates the consumption of carboxylic acid ends of COMA. The reduction in intensity of the peak just above 3000 implies the consumption of maleate vinyl protons. The carbonyl stretch appears at 1731, there are several different fatty acid chains in adduct, they all overlap to show only one peak. The peak at 1644 shows that there are still unsaturated sites of which polymerization did not go into completion possibly due to steric effects and immobility as the reaction proceeds. The fatty acid unsaturation of COMA is expected to be quite unreactive. Maleate double bonds are known not to homopolymerize and the large AESO molecule is probably too slow to diffuse and make the acrylate groups available. However, when the final sample was extracted with dichloromethane, no unreacted AESO could be isolated indicating that self-polymerization of AESO takes place readily (14).

4.5.2. Mechanical Properties

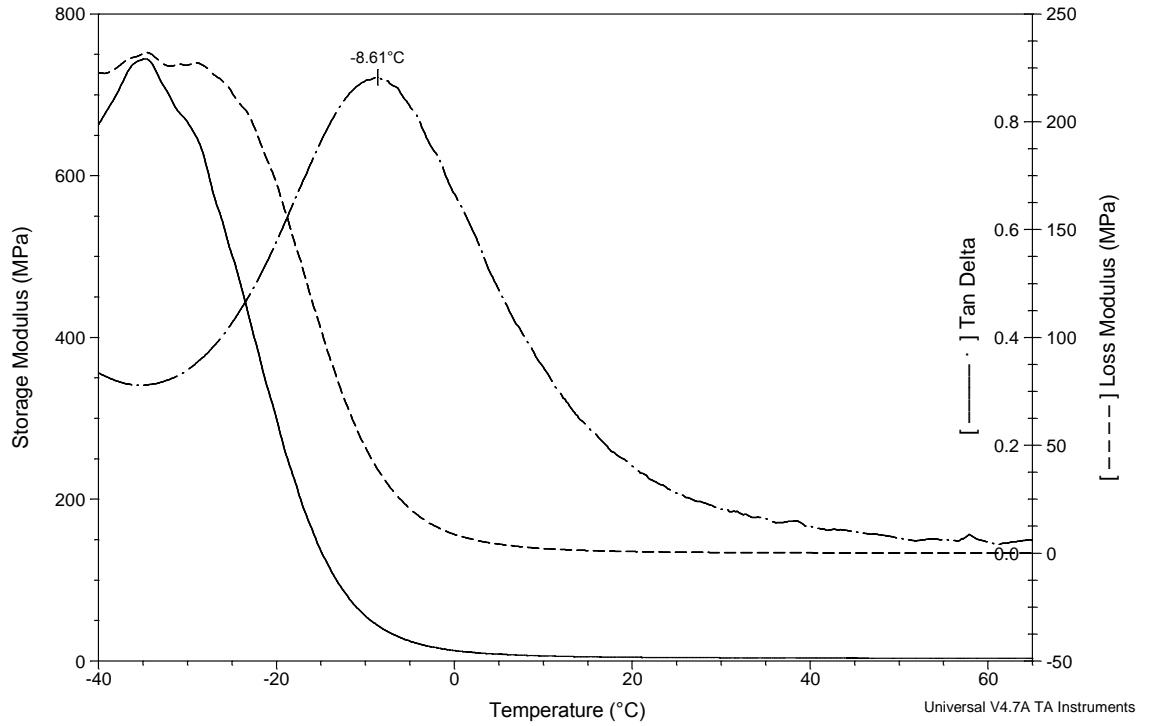


Figure 4.24. DMA Graph of AESO-X 1.5 : 0.15.

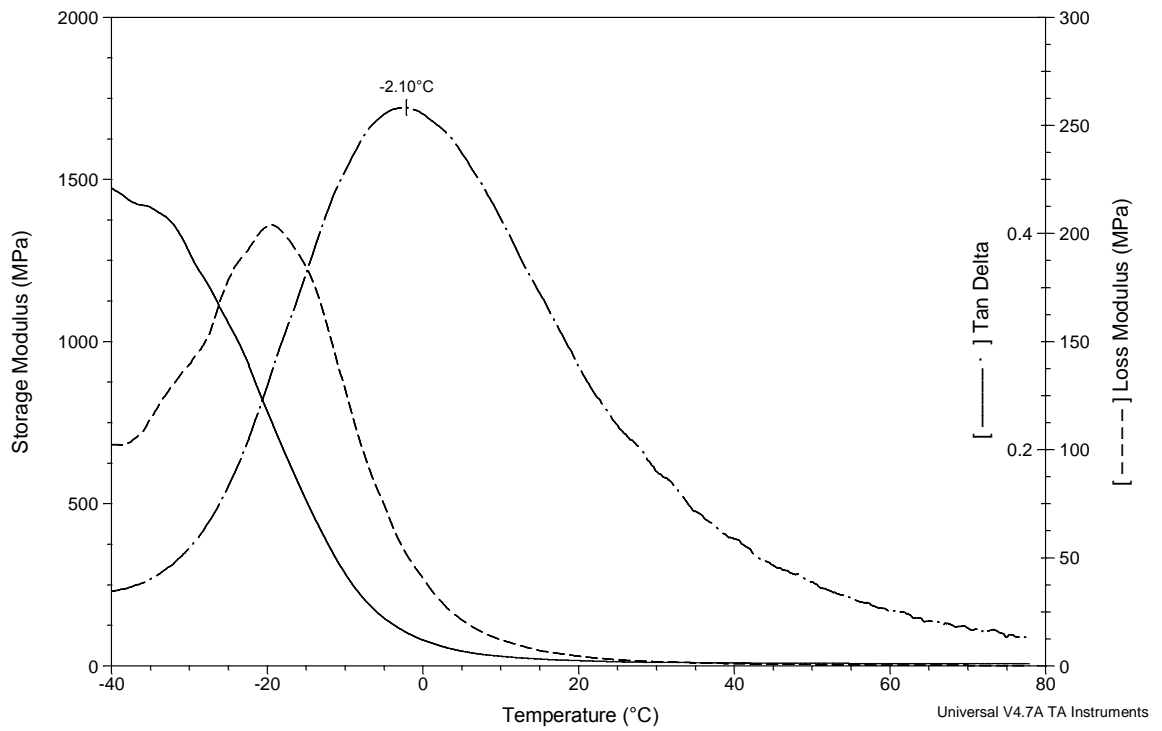


Figure 4.25. DMA Graph of AESO-X 1.5 : 0.30.

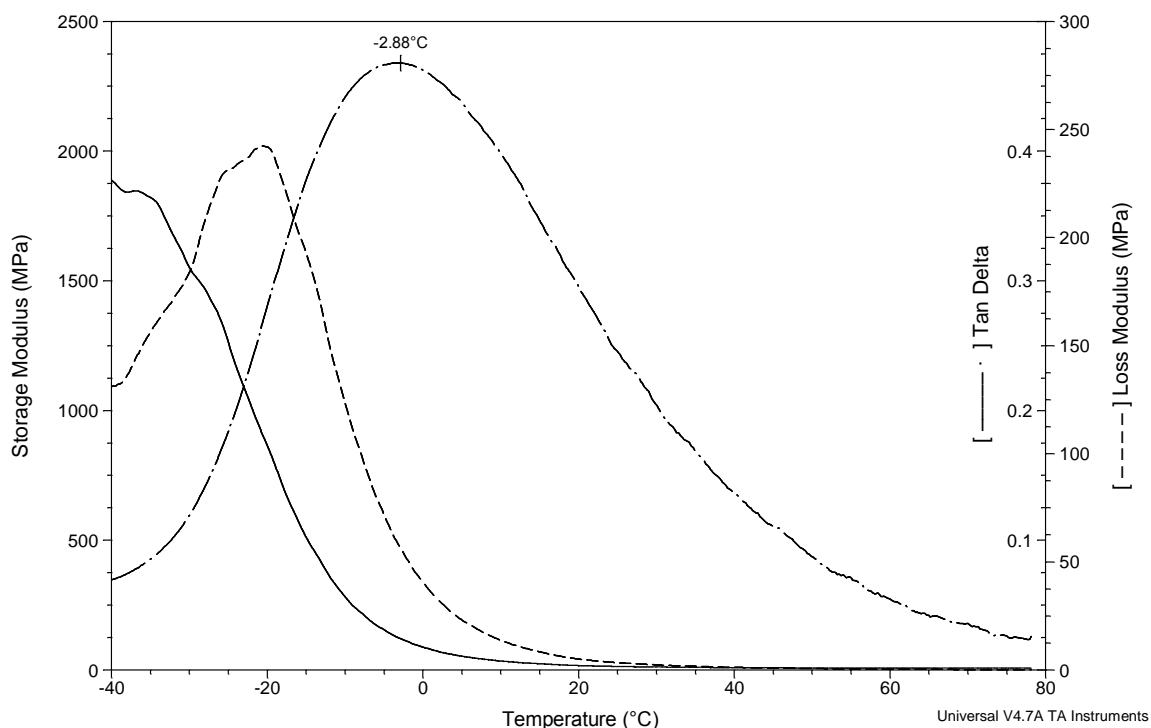


Figure 4.26. DMA Graph of AESO-X 1.5 : 0.40.

The DMA graphs of AESO-X adducts give T_g values of -8.61 , -2.10 , -2.88 °C with increasing AESO compositions. The same trend is also observed for storage modulus values as given in Figure 4.8. below. The introduction of a second network formed by COMA maleate and AESO acrylate double bonds increases the glass transition temperature and storage modulus values as expected. However, when AESO composition is increased above 30% by weight, the effect of increase in mechanical properties diminishes. Such a trend could be attributed to the stoichiometric constraints as well as the un-reacted sites of triglycerides in adduct, due to decrease in immobility and diffusivity as the reaction proceeds. All three monomers in this adduct are triglyceride chains with additional functionalities and during reaction the molecular weight increase is very rapid since only addition of one macromonomer adds around 1000 to the molecular weight of the growing molecule. Similarly, the increase in viscosity is also very rapid preventing the reactive ends of the triglycerides from coming together and reacting further. In other words, the conversion is diffusion controlled and the un-reacted sites give the adduct increased flexibility and decreased T_g .

Although AESO enhances the mechanical properties of ESOCOMA network, the T_g and storage modulus values are still low when compared to styrene adducts, which is an expected result considering that styrene reacted segments will give a rigidity which cannot be obtained with large monomers. However, AESO-X adduct is unique in the sense that all monomers are oil based, where two are derived from the same triglyceride, and except for the free radical initiator there is no additive, no co-monomer, and still the adducts obtained have acceptable mechanical properties. Among the 600 new polymers synthesized from plant oil triglycerides over the last 10 years by our research group this polymer has the highest triglyceride content. In those adducts, only the maleate and acrylate modifications on the triglycerides are the non-oil-based portions. Using the average molecular weights for the components, the oil content of the samples are calculated to be 82.5%, 81.3%, and 80.5% for the samples AESO-X 1.5 : 0.15, AESO-X 1.5 : 0.30, AESO-X 1.5 : 0.40 respectively.

Table 4.7. Result of mechanical analysis for AESO-X (8) Adducts.

	T_g (°C) DMA	Storage Modulus (MPa)*	Storage Modulus at 25 °C (MPa)
ESOCOMA (4)	-16.5	5.1	2.1
AESO-X 1.5 : 0.15	-8.6	28.2	4.3
AESO-X 1.5 : 0.30	-2.1	160.7	12.8
AESO-X 1.5 : 0.40	-2.9	165.8	13.8

* The average storage modulus at [-10-0] °C.

4.6. Comparison of Thermal Properties for all adducts

Thermal properties of adducts were determined via DSC analysis. However, considering the fact that the slope changes are not very distinct, it is not possible to observe the effect of changes in styrene or AESO compositions, thus, only one adduct from each group, namely ESOCOMA, selfX, Styrene-X, AESO-X, are subjected to DSC analysis.

The DSC traces are shown in Figure 4.25, where the lowest T_g value belongs to ESOCOMA, and the T_g increases with the increase in crosslinking density and the introduction of new monomers to form another networks. The thermal analysis for styrene-containing-adduct continued till 140 °C in order to observe the T_g of polystyrene which may appear around 80 °C -100 °C, but no such transition is observed. We can conclude that the network contains no or negligibly little styrene homopolymer segments. It is well known that the reactivity ratios of styrene and maleate lead to alternating copolymers under radical initiation. It should be noted that there is no data loss due to truncation in the graph given below.

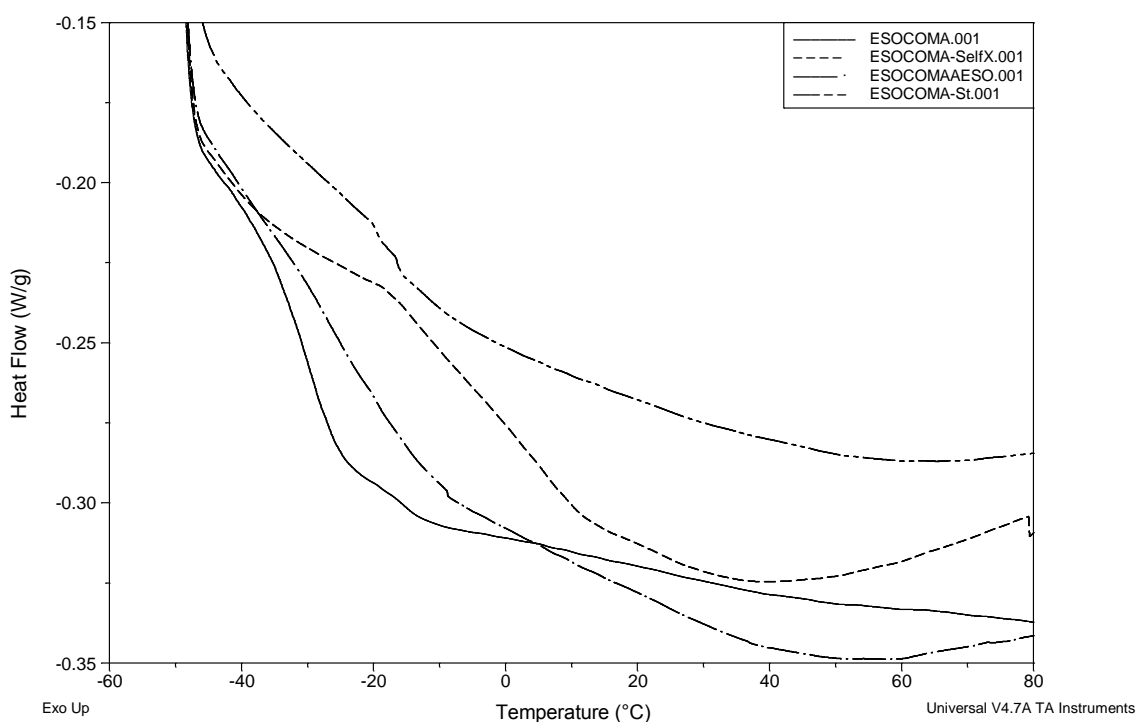


Figure 4.27. DSC Analysis graph for all adducts.

4.7. Reaction of COMA with commercial epoxy resins

Considering the fact that the use of COMA as epoxy curing agent with ESO has yielded plausible results, COMA was reacted with commercial epoxy resins such as Duratek DT 1000 and a bisphenol A diglycidyl ether and Heloxy 505 which is a castor oil

triglycidyl ether type epoxy resin. Excellent thermosets were obtained in each case. The studies on determination of the optimum stoichiometry with different commercial epoxy resins for the best mechanical properties are currently in progress. The use of COMA as an epoxy curing agent is novel and a patent application is being considered.

5. CONCLUSION

In the study, maleation of castor oil is carried out to obtain an α - β unsaturated carboxylic acid end to act as an epoxy curing agent, which can also undergo free radical reactions with polymerizable vinyl group bearing monomers due to the presence of maleate double bonds. Maleation of castor oil is known, the procedure used is very similar to those studies except for some modifications to increase yield and conversion. The maleated castor oil (COMA) is then reacted with epoxidized soybean oil (ESO) to give a thermoset polymer ESOCOMA to set an example to epoxy curing functionality of COMA. Another adduct is obtained by carrying out the free radical polymerization of maleate vinyl groups, together with the epoxy curing reaction. At the end of the free radical reaction, a doubly crosslinked network which is only composed of two functionalized triglycerides is obtained. Furthermore, with the introduction of reactive diluents capable of undergoing free radical reactions, two simultaneous semi-interpenetrating networks are formed. One of the reactive diluents was styrene, and the other was the acrylated epoxidized soybean oil (AESO). The latter is another functionalized form of ESO that can undergo radical reactions due to acrylate functionality.

The products obtained from these reactions are all insoluble in common organic solvents so the characterization was done only by FTIR. The thermal and mechanical tests such as DSC (Differential Scanning Calorimetry) and DMA (Dynamic Mechanical Analysis) were done to further analyze the properties of the thermosets. In order to determine the optimized value for ESO/COMA, surface hardness values measured by durometer were used whereas the effects of compositions of styrene and AESO monomers were analyzed according to DMA data.

The use of COMA as a multifunctional curing agent for commercially available epoxy resins gave clear, tough, high tensile strength thermosets. Optimization and characterization of these compounds with the intent of commercialization, is underway.

REFERENCES

1. Can, E., S. H. Küsefoğlu and R. Wool, "Soybean and Castor Oil Based Thermosetting Polymers: Mechanical Properties", *Journal of Applied Polymer Science*, Vol. 102, pp. 1497-1504, 2006.
2. Lligadas, G. I. P., *Biobased Thermosets from Vegetable Oils Synthesis, Characterization, and Properties*, Ph. D. Thesis, Universitat Rovira I Virgili, 2006.
3. Gunstone, F., "Fatty Acid and Lipid Chemistry", New York: Blackie Academic and Professional, 1996.
4. Naughton, F. C., F. Dunczky, C. R. Swenson and T. Kroplinski, *Kirk Othmer Encyclopedia of Chemical Technology*. New York : John Wiley and Sons, 1979.
5. "Comprehensive Castor Oil Report Preview", <http://www.castoroil.in>, accessed at May 2010.
6. Tran, N. B., J. Vialle and Q. T. Pham, "Castor oil-based polyurethanes: 2. Tridimensional polyaddition in bulk between castor oil and diisocyanates-gelation and determination of Fw(OH)", *Polymer*, pp. Vol. 38 No. 13, pp. 3307-3314, 1997.
7. Tran, N. B., J. Vialle and Q. T. Pham, "Castor oil-based polyurethanes: 1. Structural characterization of castor oil nature of intact glycerides and distribution of hydroxyl groups", *Polymer*, pp. Vol. 38 No. 10, pp. 2467-2473, 1997.
8. Sharma, V., P. P. Kundu, "Addition polymers from natural oils—A review", *Progress in Polymer Science*, pp. 983–1008, 2006.
9. Dasari, M. A., *Reaction Engineering Options for Producing Biodiesel and Cetane Improvers from Fats and Oils.*, University of Missouri, Columbia, 2003.
10. Öztürk, C., *Polymerization Reactions of Functionalized Vegetable Oils With Petroleum Based Macromonomers*, Ph. D. Thesis, Boğaziçi University, 2010.

11. Meher, L. C., D. V. Sagar and S. N. Naik, "Technical aspects of biodiesel production by transesterification—a review", *Renewable and Sustainable Energy Reviews*, Vol. 10, pp. 248-268, 2006.
12. Rios, L. A., *Heterogeneously Catalyzed Reactions with Vegetable Oils: Epoxidation and Nucleophilic Epoxide Ring-Opening with Alcohols.*, Ph. D. Thesis, Rheinisch-Westfälischen Technischen Hochschule, 2003.
13. Karmalm, P., T. Hjertberg, A. Jansson, R. Dahl and K. Ankner, "Network formation by epoxidised soybean oil in plastisol poly(vinyl chloride)", *Polymer Degradation and Stability*, Vol. 94, pp. 1986-1990, 2009.
14. Wool, R. P., S. H. Küsefoğlu, G. Palmese, S. Khot and R. Zhao, "High Modulus Polymers and Composites from Plant Oils", U. S. Patent 6,121,398 (2000).
15. Lu, J., S. Khot and R. P. Wool, "New sheet molding compound resins from soybean oil I. Synthesis and characterization", *Polymer*, pp. 71-80, 2005.
16. Öztürk, C., H. Mutlu, M. A. R. Meier and S. H. Küsefoğlu, "4-Vinylbenzenesulfonic acid adduct of epoxidized soybean oil: Synthesis, free radical and ADMET polymerizations", *European Polymer Journal*, Vol. 47, pp. 1467–1476, 2011.
17. Wallenberger, F. T., N. E. Weston, *Natural Fibers, Plastics and Composites*. s.l. : Springer, Kluwer Academic Publishers, 2004.
18. Eren, T., *Synthesis Of New Polymers From Plant Oil Triglycerides*, Ph.D. Thesis, Boğaziçi University, İstanbul, Turkey, 2004.
19. Can, E., S. H. Küsefoğlu and R. Wool, "Soybean and Castor Oil Based Monomers: Synthesis and Copolymerization with Styrene", *Journal of Applied Polymer Science*, Vol. 102, pp. 2433-2447, 2006.
20. Wang, H. J., M. Z. Rong, M. Q. Zhang, J. Hu, H. W. Chen and T. Czigany, "Biodegradable Foam Plastics Based on Castor Oil", *Biomacromolecules*, pp. 615–623, 2008.

21. Bertz, S. T., F. M. Miksza and E. Zucker, "High Purity Adduct of Castor Oil", 6,225,485 (1999).
22. Taylan, E., S. H. Küsefoğlu, "Chain Extension Reactions of Unsaturated Polyesters with Epoxy Compounds", *Journal of Applied Polymer Science*, Vol. 112, pp. 1184-1191, 2009.
23. Esen, H. and S. H. Küsefoğlu, "Photolytic and Free Radical Polymerization of Cinnamate Esters of Epoxidized Plant Oil Triglycerides", *Journal of Applied Polymer Science*, Vol. 89, pp. 3882-3888, 2003.
24. Esen, H., S. H. Küsefoğlu and R. Wool, "Photolytic and Free-Radical Polymerization of Monomethyl Maleate Esters of Epoxidized Plant Oil Triglycerides", *Journal of Applied Polymer Science*, Vol. 103, pp. 626-633, 2007.
25. Esen, H., S. H. Küsefoğlu and R. Wool, "Photolytic and Free Radical Polymerization of Epoxidized Plant Oil Triglycerides", *Polymer Preprints*, Vol. 45, pp. 577-578, 2004.
26. Narine, S. S., X. Kong, "Vegetable Oils in Production of Polymers and Plastics", *Macromolecules*, pp. 299-302, 2005.
27. Odian, G., *Principles of Polymerization*, 4th Edition, Wiley&Sons Inc, pp. 143, 527, 2004.